IEEE Access
Multidisciplinary : Rapid Review : Open Access Journal

Received March 19, 2020, accepted April 20, 2020, date of publication May 6, 2020, date of current version May 15, 2020.

Digital Object Identifier 10.1109/ACCESS.2020.2991847

Joint Relay Selection, Full-Duplex and Device-to-Device Transmission in Wireless Powered NOMA Networks

HUU-PHUC DANG[1,2], MINH-SANG VAN NGUYEN[3], DINH-THUAN DO[4], HONG-LIEN PHAM[1], BASSANT SELIM[5], (Member, IEEE), AND GEORGES KADDOUM[5]

[1]Faculty of Electrical and Electronics Engineering, Ho Chi Minh City University of Technology and Education, Ho Chi Minh City 700000, Vietnam
[2]Electrical - Electronics Department, School of Engineering and Technology, Tra Vinh University, Tra Vinh 87000, Vietnam
[3]Faculty of Electronics Technology, Industrial University of Ho Chi Minh City (IUH), Ho Chi Minh City 71406, Vietnam
[4]Wireless Communications Research Group, Faculty of Electrical & Electronics Engineering, Ton Duc Thang University, Ho Chi Minh City 758307, Vietnam
[5]Electrical Engineering Department, ETS, University of Quebec, Montreal, QC H3C 1K3, Canada

Corresponding author: Dinh-Thuan Do (dodinhthuan@tdtu.edu.vn)

ABSTRACT This paper investigates non-orthogonal multiple access (NOMA), cooperative relaying, and energy harvesting to support device-to-device (D2D) transmission. In particular, we deploy multiple relay nodes and a cell-center D2D device which can operate in full-duplex (FD) or half-duplex (HD) mode to communicate with a cell-edge D2D device. In this context, there are two possible signal transmission paths from the base station (BS) to the far D2D user either through multiple decode-and-forward (DF) relay nodes or through a near D2D user. Consequently, we propose three schemes to support D2D-NOMA systems, namely non-energy harvesting relaying (Non-EHR), energy harvesting relaying (EHR) and quantize-map-forward relaying (QMFR) schemes. For each of the proposed schemes, closed-form expressions of the outage probabilities of both D2D users are derived. Extensive Monte-Carlo simulation results are provided to validate the derived analytical expressions. The study results show that the proposed schemes can improve the outage performance compared to conventional orthogonal multiple access (OMA) schemes. Moreover, it is shown that the Non-EHR scheme achieves the best outage performance among the three considered schemes.

INDEX TERMS Device-to-device, full-duplex, non-orthogonal multiple access, relay selection.

I. INTRODUCTION

The emerging non-orthogonal multiple access (NOMA) scheme is attracting considerable attention due to its capacity to support massive connectivity in numerous applications including multimedia applications and the Internet of Things (IoT) [1]. It was demonstrated that NOMA is superior to conventional orthogonal multiple access (OMA)schemes in terms of system throughput [2]. The main advantage is that NOMA achieves greater overall throughput than OMA methods in both uplink and downlink. Moreover, NOMA can be employed in relay networks to improve coverage [3]. In contrast to the traditional waterfilling scheme, to ensure user fairness, NOMA allocates more power to the clients with weaker channel conditions [4]. In addition, NOMA also provide higher reliability and achieves higher fairness among users thanks to combining with relaying techniques schemes [5]–[7]. Since NOMA systems benefit from low latency, improved system throughput, and fairness, NOMA has become very attractive where it is considered a strong candidate with the famous Orthogonal Frequency Division Multiple-Access (OFDMA) to 5G wireless network [8]. Therefore, the authors in [9] focused on relay selection techniques based on the NOMA principle. The research results demonstrated that joint cooperative relaying and NOMA can incredibly enhance the system's performance compared to traditional OMA. Also, considering relay selection in NOMA systems, the research work in [10] has achieved interesting results in finding asymptotic and approximate expressions to the average sum rate in Amplify-and-Forward (AF) mode. In addition, another relay selection method based on partial channel state information (CSI) was proposed in [11]. Besides, assuming different NOMA relaying modes such as AF [12] and Decode-and-Forward (DF) [13], the authors

The associate editor coordinating the review of this manuscript and approving it for publication was Xujie Li.

in [14] introduced a relaying protocol called quantize-map-forward (QMF), adopted in NOMA to forward information. However, the above studies mostly use half-duplex (HD) technology, which is characterized by a limited spectrum efficiency. On the other hand, FD technology can be used to increase spectral efficiency in cellular networks [15]–[18].

To meet the requirements of explosive data traffic in 5G networks, ultra-dense heterogeneous networks are considered as a prominent technique [19]. In heterogeneous networks, device-to-device (D2D) communications is proposed as a promising solution for mobile data offloading in wireless networks, for enhancing the spectral efficiency of cellular networks, and for increasing the mobility without the help of base stations [20]. Moreover, D2D can be applied as an effective solution to support neighborhood based services such as social networking and data sharing when the devices are in close vicinity [20]. Although D2D communication has many benefits in cellular networks, the D2D users also interfere with each other. Therefore, interference management and energy efficiency are critical in D2D networks in order to minimize interference and increase the battery lifetime of the user equipment (UE) [21].

The combinations of D2D and NOMA yields promising outcomes that have been shown in [22] where the authors proposed a new approach based on combining the NOMA-based D2D users into groups that can share the same sub-channels. In this context, the near user device can act as a relay node which assists the base station (BS) to transmit information to the far device [23]. In a similar study [24], the authors maximized the total rate of the D2D-NOMA system by proposing a joint sub-channel and power allocation scheme that satisfies the signal-to-interference-plus-noise ratio (SINR) requirements of all D2D users in the network. Furthermore, the resource allocation problem, based on joint subchannel and user pairing, and power control in NOMA D2D networks has been addressed in [25].

It is noted that the battery lifetime budget of users limits the system throughput performance in D2D underlaid cellular networks. Fortunately, in order to prolong the network lifetime, D2D underlaid cellular networks can benefit from energy harvesting [26]–[30]. The authors in [29] studied NOMA-based cellular networks allowing the energy harvesting-powered D2D devices to share the downlink resources of the cellular network. The energy harvesting constraints on the D2D links were investigated and the average energy efficiency of D2D links was maximized in [30].

A. MOTIVATION AND OUR CONTRIBUTIONS

Despite the reported advantages of NOMA and D2D schemes in recent works, several open problems need to be addressed in terms of energy efficiency, improving performance of far device, FD transmission, and transmit antenna selection (TAS). In this context, the authors in [31] presented the optimal performance of the D2D communication by jointly optimizing the power allocation and the resource block assignment. They introduced a distributed decision making (DDM) framework for NOMA systems by considering the successive interference cancellation (SIC) decoding order related to the NOMA-based cellular users. In [32], to minimize interference in hybrid D2D and cellular networks, a NOMA-assisted coordinated direct and relay transmission was proposed to fully achieve the inherent characterization of NOMA. Their proposed system further provided a potential scheme for hybrid networks to enhance the spectral efficiency and cell coverage. Motivated by the results in [23], [32], to improve the performance of D2D users, this paper studies three schemes for relay selection assisted D2D-NOMA systems by relying on transmit antenna selection and FD transmission. The main contributions of this paper are summarized as follows:

1) Different from [23], we propose three new D2D-NOMA communication network models. In addition, the combination with relay selection, TAS and energy harvesting to enhance performance of the cell-edge device and then spectral efficiency is also improved.
2) We derive exact expressions for the outage probability and system throughput of the three proposed schemes. The outage performance of the considered system in Scheme 1 is confirmed as the best case among three cases.
3) The derived expressions are validated via Monte Carlo simulations to corroborate the exactness of the analysis. Several important parameters that affect the system's performance are considered and outage performance comparisons of the three schemes are presented to elaborate on their respective performances.

B. ORGANIZATION

The rest of this paper is structured as follows. The system model and the related assumptions of the three schemes are detailed in Section 2. Next, the outage probability analysis of the three schemes is presented in Section 3. Based on the analytical results of the outage probability, the system's throughput is analyzed in section 4. Simulation results are presented in Section 5 while Section 6 concludes this work.

II. SYSTEM MODEL

We consider a downlink cellular system, depicted in Fig. 1, consisting of a base station (BS), D2D link containing the cell-center device D_1 and the cell-center device D_2. To robust signal transmission to the cell-edge device D_2, it is required K decode-and-forward (DF) relaying nodes. In this NOMA scenario, the BS is equipped with N antennas and is able to directly communicate with the cell-center device D_1 while the cell-edge device D_2 is served by D_1 and the selected relay. We assume that there is no direct link from BS to D_2 due to deep fading or obstacles. In this context, it is assumed that the FD-assisted relays are equipped with a pair of antennas, one for transmitting while the other is serving the purpose of receiving. Meanwhile, to enhance the transmission quality, only the best antenna at the BS and the best relay are selected

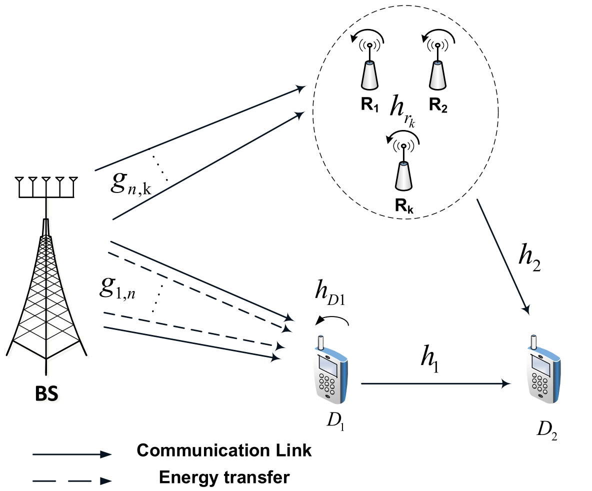

FIGURE 1. System model of joint relay selection and FD in D2D-NOMA systems.

to transmit the signal dedicated to D_2. In addition, D_1 also acts as a relay node that supports D2D transmission of signals from the BS to D_2 [23]. It is worth noting that D_1 and the relays are assumed to be able to switch the operating state from FD to HD mode and vice versa. On the other hand, the relays only serve for data transfer from the BS to D_2 and they are not assigned to serve D_1. In this scenario, let $g_{1,n}, g_{n,k}$ ($k = 1, 2, \ldots, K$ and $n = 1, 2, \ldots, N$), h_1, and h_2 denote the Rayleigh fading channel coefficients of the $BS \rightarrow D_1$, $BS \rightarrow R_k$, $D_1 \rightarrow D_2$, and selected $Relay \rightarrow D_2$, respectively. Consequently, the channel gains $\left|g_{1,n}\right|^2$, $\left|g_{n,k}\right|^2$, $|h_1|^2$, and $|h_2|^2$ are independent exponential random variables with parameters $\lambda_{g1,n}$, $\lambda_{gn,k}$, λ_{h1}, and λ_{h2}, respectively. Moreover, since D_1 and the relays are equipped with two antennas and they can work in FD mode, we denote $h_{D1} \sim CN(0, \lambda_{hD1})$ and $h_{r_k} \sim CN(0, \lambda_{hr_k})$ are the Rayleigh distributed feedback channel coefficients of the loop self-interference (SI) at D_1 and R_k, respectively.[1]

According to the principle of NOMA, the BS sends the superimposed NOMA signal $x_S^{NOMA} = \sqrt{a_1 P_S}x_1 + \sqrt{a_2 P_S}x_2$ to the k^{th} relay and D_1, where x_1 and x_2 are the messages intended for D_1 and D_2, respectively. Here, a_1, a_2 ($i = 1, 2$) are the power allocation coefficients of the two devices D_1, D_2 respectively and these terms satisfying conditions, i.e. $a_2 > a_1 > 0$ and $a_1 + a_2 = 1$. Moreover, P_S, P_R, and P_1 are the transmission powers at the BS, the relays, and D_1, respectively. In this paper, we also denote the additive white Gaussian noise (AWGN) at the relay, devices in the network by $w_j \sim CN(0, \sigma_0^2)$, where ($j = 1, \ldots, 4$).

In the following subsections, we consider three possible scenarios for the proposed D2D NOMA scheme where D_1 can operate without energy harvesting (Non-EHR), with energy harvesting (EHR), and by applying the quantize-map-forward relaying (QMFR) protocol.

A. SCHEME 1: NON-ENERGY HARVESTING RELAYING

In this situation, D_1 does not harvest energy from the BS. In this context, from its N antennas, the BS will select the best channel to transmit the signal to device D_1 and the K relays. For the best link from $BS \rightarrow D_1$ and $BS \rightarrow R_k$, the best antenna of BS can be selected by the following criterion [34]

$$n^* = \arg \max_{n=1,\ldots N} \left(|g_x|^2\right), \tag{1}$$

where $x = \{(1, n) \;\; or \;\; (n, k)\}$.

In the Non-EHR scheme, the received signal at D_1 is given by

$$\begin{aligned} y_{SD1}^{NOMA} &= g_{1,n^*} x_S^{NOMA} + w_1 \\ &= g_{1,n^*}\left(\sqrt{a_1 P_S}x_1 + \sqrt{a_2 P_S}x_2\right) \\ &\quad + h_{D1}\sqrt{\omega P_1}x_{D1} + w_1, \end{aligned} \tag{2}$$

where x_{D1} denotes the loop interference signal of D_1, ω represents the FD/HD operation factor to indicate FD or HD activated at D_1 and R_k, i.e., $\omega = 1$ and $\omega = 0$ correspond to the FD and HD mode, respectively. Likewise, the received signal at the k^{th} relay is given by

$$\begin{aligned} y_{SRK}^{NOMA} &= g_{n^*,k} x_S^{NOMA} + w_2 \\ &= g_{n^*,k}\left(\sqrt{a_1 P_S}x_1 + \sqrt{a_2 P_S}x_2\right) \\ &\quad + h_{r_k}\sqrt{\omega P_R}x_r + w_2, \end{aligned} \tag{3}$$

where x_r denotes the loop interference signal of relay R_k. In the second hop, the best path among the relays and D_1 is selected to forward the message to D_2. If the best path corresponds to a relay, R_k decodes the received signal from the BS and forwards the message with power P_R to D_2. The received signal at D_2 is expressed by

$$y_{SRKD_2}^{NOMA} = h_2\sqrt{P_R}x_2 + w_3. \tag{4}$$

Regarding D2D link, D_1 forwards x_2 to D_2. Thus, the received signal at D_2 is expressed as

$$y_{D_{12}}^{NOMA} = h_1\sqrt{P_1}x_2 + w_4. \tag{5}$$

Precisely, after receiving the signal from BS, D_1 performs SIC to decode his message, i.e., it decodes x_2, subtracts it from the received signal and then decodes its own message x_1. Thus, the instantaneous signal to interference plus noise ratio at D_1 to decode x_2 is given as

$$\begin{aligned} \gamma_{SD1\leftarrow 2}^{NOMA} &= \frac{a_2 P_S\left|g_{1,n^*}\right|^2}{a_1 P_S\left|g_{1,n^*}\right|^2 + \omega P_1|h_{D1}|^2 + \sigma_0^2} \\ &= \frac{a_2\rho\left|g_{1,n^*}\right|^2}{a_1\rho\left|g_{1,n^*}\right|^2 + \omega\rho|h_{D1}|^2 + 1}, \end{aligned} \tag{6}$$

[1] Similar with system model reported in [23], we focus on the performance improvement of the cell-edge device in D2D-NOMA systems. It is assumed that sophisticated channel estimation algorithms have been acquired with sufficient training information to obtain perfect CSI. Regarding FD, loop back signals still exist in the receiver due to imperfect interference cancellation

where $\rho = \frac{P_S}{\sigma_0^2}$ is the transmit signal-to-noise ratio (SNR). Without loss of generality, it is assumed that P_S, P_R, and P_1 are the normalized transmission power at the BS, relays, and D_1, respectively. Assuming perfect SIC, the instantaneous SINR for decoding x_1 at D_1 is given as

$$\gamma_{SD1}^{NOMA} = \frac{a_1\rho|g_{1,n^*}|^2}{\omega\rho|h_{D1}|^2+1}. \tag{7}$$

Thus, if the $D_1 \to D_2$ link is stronger than the $R_k \to D_2$ link, D_2 will receive its signal x_2 from D_1. In this case, the received SINR at D_2 is given by

$$\gamma_{D12,x2}^{NOMA} = \frac{P_1|h_1|^2}{\sigma_0^2} = \rho|h_1|^2. \tag{8}$$

Meanwhile, the instantaneous SINR at relay R_k for detecting x_2 is evaluated as

$$\begin{aligned}\gamma_{SRK,x2}^{NOMA} &= \frac{a_2P_S|g_{n^*,k}|^2}{a_1P_S|g_{n^*,k}|^2+\omega P_r|h_{r_k}|^2+\sigma_0^2}\\ &= \frac{a_2\rho|g_{n^*,k}|^2}{a_1\rho|g_{n^*,k}|^2+\omega\rho|h_{r_k}|^2+1}.\end{aligned} \tag{9}$$

Therefore, considering the link $R_k \to D_2$, the instantaneous SINR at D_2 is given by

$$\gamma_{RKD2,x2}^{NOMA} = \frac{P_R|h_2|^2}{\sigma_0^2} = \rho|h_2|^2. \tag{10}$$

Regarding relay link, if the signal is transmitted from the BS to D_2 with the help of relay nodes, the best relay node is selected by the following criterion

$$k^* = \arg\max_{k=1,\cdots,K}\min\left(\gamma_{SRK,x2}^{NOMA}, \gamma_{RKD2,x2}^{NOMA}\right). \tag{11}$$

In addition, the instantaneous SINR at relay R_k for detecting x_2 is evaluated as

$$\begin{aligned}\gamma_{SRK,x2}^{NOMA} &= \frac{a_2P_S|g_{n^*,k}|^2}{a_1P_S|g_{n^*,k}|^2+\omega P_r|h_{r_k}|^2+\sigma_0^2}\\ &= \frac{a_2\rho|g_{n^*,k}|^2}{a_1\rho|g_{n^*,k}|^2+\omega\rho|h_{r_k}|^2+1}.\end{aligned} \tag{12}$$

Therefore, considering the link $R_k \to D_2$, the instantaneous SINR at D_2 is given by

$$\gamma_{RKD2,x2}^{NOMA} = \frac{P_R|h_2|^2}{\sigma_0^2} = \rho|h_2|^2. \tag{13}$$

Therefore, the instantaneous SINR at user D_2 is written as

$$\begin{aligned}\gamma_{D2}^{NOMA} = max\Big(&\min\left(\gamma_{SD1\leftarrow2}^{NOMA}, \gamma_{D12,x2}^{NOMA}\right),\\ &\max_{k=1,\cdots,K}\min\left(\gamma_{SRK,x2}^{NOMA}, \gamma_{RKD2,x2}^{NOMA}\right)\Big).\end{aligned} \tag{14}$$

B. SCHEME 2: ENERGY HARVESTING RELAYING (EHR)

In this scheme, D_1 harvests energy from the BS in the first phase and uses such energy to transmit the signal to D_2 in the second phase. We assume that the energy obtained from the noise is very small and it can be ignored. Therefore, according to the power splitting protocol (PS) [33] for energy harvesting, the received signal at D_1 in the first phase is expressed as

$$\begin{aligned}y_{SD1}^{NOMA-EH} &= \sqrt{(1-\beta)}g_{1,n^*}\left(\sqrt{a_1P_S}x_1+\sqrt{a_2P_S}x_2\right)\\ &\quad + h_{D1}\sqrt{\omega P_1}x_{D1}+w_1,\end{aligned} \tag{15}$$

where $\beta \in (0, 1)$ is the power splitting ratio. Therefore, the SINR at D_1 to decode x_2 is given by

$$\gamma_{SD1\leftarrow2}^{NOMA-EH} = \frac{(1-\beta)a_2\rho|g_{1,n^*}|^2}{(1-\beta)a_1\rho|g_{1,n^*}|^2+\omega\rho|h_{D1}|^2+1}. \tag{16}$$

Assuming perfect SIC, the SINR for decoding x_1 at D_1 is given by

$$\gamma_{SD1}^{NOMA-EH} = \frac{(1-\beta)a_1\rho|g_{1,n^*}|^2}{\omega\rho|h_{D1}|^2+1}. \tag{17}$$

Applying the PS protocol, the harvested energy is obtained as

$$E = \frac{T}{2}\eta\beta\left(P_s|g_{1,n^*}|^2+P_1|h_{D1}|^2\right), \tag{18}$$

where $0 < \eta < 1$ is the energy conversion coefficient and T is the block time. Then, the transmit power $\frac{E}{T/2}$ at D_1 can be expressed as

$$P_1 = \frac{\eta\beta P_s|g_{1,n^*}|^2}{1-\eta\beta|h_{D1}|^2}. \tag{19}$$

It is noted that the condition $|h_{D1}|^2 < \frac{1}{\eta\beta}$ must be satisfied. Hence, the SINR for D_2 to detect x_2 is given by

$$\gamma_{D12,x2}^{NOMA-EH} = \frac{\eta\beta\rho|g_{1,n^*}|^2|h_1|^2}{1-\eta\beta|h_{D1}|^2}. \tag{20}$$

It is noted that the criterion for selecting the best antenna at the BS and the relays in this case is the same as in Scheme 1, i.e., the expressions in (1) and (11), respectively.

C. SCHEME 3 (QMFR)

In contrast to Scheme 1 and Scheme 2, D_1 applies the QMFR protocol [19] to decode its own information and then subtracts it from the superposed signal in the first phase. In this case, the SINR at D_1 to decode x_1 in the case of without energy harvesting at D_1 can be expressed as

$$\gamma_{SD1}^{QMF} = \frac{a_1\rho|g_{1,n^*}|^2}{a_2\rho|g_{1,n^*}|^2+\omega\rho|h_{D1}|^2+1}. \tag{21}$$

Following the cancellation of x_1, the signal intended for D_2 is decoded and re-transmitted to D_2 via D_1. In this case, the SINR at D_1 to detect x_2 can be expressed as

$$\gamma_{SD1,x2}^{QMF} = \frac{a_2\rho\left|g_{1,n^*}\right|^2}{\omega\rho|h_{D1}|^2 + 1}. \tag{22}$$

For the case of energy harvesting at D_1, the SINR at D_1 for decoding x_1 is calculated as

$$\gamma_{SD1}^{QMF-EH} = \frac{(1-\beta)\,a_1\rho\left|g_{1,n^*}\right|^2}{(1-\beta)\,a_2\rho\left|g_{1,n^*}\right|^2 + \omega\rho|h_{D1}|^2 + 1}, \tag{23}$$

and the SINR at D_1 to detect x_2 can be expressed as

$$\gamma_{SD1,x2}^{QMF-EH} = \frac{(1-\beta)\,a_2\rho\left|g_{1,n^*}\right|^2}{\omega\rho|h_{D1}|^2 + 1}. \tag{24}$$

Similarly, the relays employ the QMFR protocol to decode x_1 and x_2. Hence, the instantaneous SINR at R_k for detecting x_1 and x_2 can be calculated as

$$\gamma_{SRK,x1}^{QMF} = \frac{a_1\rho\left|g_{n^*,k}\right|^2}{a_2\rho\left|g_{n^*,k}\right|^2 + \omega\rho\left|h_{r_k}\right|^2 + 1}, \tag{25}$$

and

$$\gamma_{SRK,x2}^{QMF} = \frac{a_2\rho\left|g_{n^*,k}\right|^2}{\omega\rho\left|h_{r_k}\right|^2 + 1}, \tag{26}$$

respectively.

Finally, in this scheme, the best relay node is also selected by the following criterion

$$k_{QMF}^{*} = \arg\max_{k=1,\cdots,K} \min\left(\gamma_{SRK,x1}^{QMF}, \gamma_{SRK,x2}^{QMF}, \gamma_{RKD2,x2}^{NOMA}\right). \tag{27}$$

III. OUTAGE PROBABILITY ANALYSIS

In this section, we investigate the outage probability of D_1 and D_2 considering the aforementioned schemes.

A. SCHEME 1

1) OUTAGE PROBABILITY OF D_1

In this case, according to the principle of NOMA, an outage event at D_1 will occur when D_1 cannot detect x_1 successfully. Therefore, the outage probability of D_1 can be expressed as

$$OP_{1-NOMA}^{FD} = 1 - \Pr\left(\gamma_{SD1\leftarrow 2}^{NOMA} \geq \varepsilon_2^{FD}, \gamma_{SD1}^{NOMA} \geq \varepsilon_1^{FD}\right), \tag{28}$$

where $\omega = 1$, $\varepsilon_1^{FD} = 2^{R_1} - 1$ is the SNR threshold, with R_1 being the target rate of D_1, while $\varepsilon_2^{FD} = 2^{R_2} - 1$, R_2 is the target rate of D_2.

Theorem 1: The outage probability of D_1 in Scheme 1 is obtained as

$$OP_{1-NOMA}^{FD} = 1 - \sum_{n=1}^{N} \binom{N}{n} (-1)^{n-1} \times \frac{\lambda_{g1,n}}{n\omega\rho\psi_1\lambda_{hD1} + \lambda_{g1,n}} \exp\left(-\frac{n\psi_1}{\lambda_{g1,n}}\right), \tag{29}$$

which is valid for $a_2 > \varepsilon_2^{FD} a_1$ and $\psi_1 = \max\left(\frac{\varepsilon_2^{FD}}{(a_2\rho - \varepsilon_2^{FD} a_1\rho)}, \frac{\varepsilon_1^{FD}}{a_1\rho}\right)$.

Proof: By substituting (6) and (7) into (28), the outage probability of D_1 is obtained as

$$\begin{aligned} OP_{1-NOMA}^{FD} &= 1 - \Pr\left(\left|g_{1,n^*}\right|^2 \geq \left(\omega\rho|h_{D1}|^2 + 1\right)\psi_1\right) \\ &= 1 - \int_0^\infty \left(1 - F_{\left|g_{1,n^*}\right|^2}((\omega\rho x + 1)\psi_1)\right) f_{|h_{D1}|^2}(x)dx. \end{aligned} \tag{30}$$

According to [34], the cumulative distribution functions (CDFs) and the probability density functions (PDFs) of the random variables $\left|g_{1,n^*}\right|^2$ and $\left|g_{n^*,k}\right|^2$ are given by

$$F_{|g_{x*}|^2}(x) = 1 - \sum_{n=1}^{N} \binom{N}{n} (-1)^{n-1} \exp\left(-\frac{nx}{\lambda_x}\right), \tag{31}$$

and

$$f_{|g_{x*}|^2}(x) = \sum_{n=1}^{N} \left(Nn\right) (-1)^{n-1} \frac{n}{\lambda_x} \exp\left(-\frac{nx}{\lambda_x}\right), \tag{32}$$

respectively. Therefore, the outage probability of D_1 is obtained as

$$\begin{aligned} OP_{1-NOMA}^{FD} &= 1 - \sum_{n=1}^{N} \binom{N}{n} (-1)^{n-1} \frac{1}{\lambda_{hD1}} \\ &\times \int_0^\infty \exp\left(-\frac{n(\omega\rho x + 1)\psi_1}{\lambda_{g1,n}}\right) \exp\left(-\frac{x}{\lambda_{hD1}}\right) dx. \end{aligned} \tag{33}$$

It is noted that the other channels, i.e., h_1, h_2 and all loop feedback channels follow the Rayleigh distribution with PDF and CDF $f_{\mathbb{X}}(x) = \frac{1}{\lambda_{\mathbb{X}}} e^{-\frac{x}{\lambda_{\mathbb{X}}}}$ and $F_{\mathbb{X}}(x) = 1 - e^{-\frac{x}{\lambda_{\mathbb{X}}}}$, respectively. Following some mathematical simplifications, the expected formula is derived. This completes the proof. □

2) OUTAGE PROBABILITY OF D_2

Because D_2 receives the signal x_2 from either D_1 or the best relay R_{k^*}, an outage event at D_2 happens if D_1 cannot successfully detect x_2 or D_2 cannot successfully decode x_2 from D_1 if the D2D link is selected. Otherwise, the outage event occurs if the best relay R_{k^*} cannot decode x_2 or D_2 cannot successfully decode the signal forwarded from the relay. Thus, the outage probability of D_2 can be formulated as

$$\begin{aligned} OP_{2-NOMA}^{FD} &= \Pr\left[\max\left(\min\left(\gamma_{SD1\leftarrow 2}^{NOMA}, \gamma_{D12,x2}^{NOMA}\right), \max_{k=1,\cdots,K} \min\left(\gamma_{SRK,x2}^{NOMA}, \gamma_{RKD2,x2}^{NOMA}\right)\right) < \varepsilon_2^{FD}\right] \\ &= \Pr\left[\min\left(\gamma_{SD1\leftarrow 2}^{NOMA}, \gamma_{D12,x2}^{NOMA}\right) < \varepsilon_2^{FD}, \max_{k=1,\cdots,K} \min\left(\gamma_{SRK,x2}^{NOMA}, \gamma_{RKD2,x2}^{NOMA}\right) < \varepsilon_2^{FD}\right]. \end{aligned} \tag{34}$$

Theorem 2: The outage probability of D_2 in Scheme 1 is obtained as (35) *and it is shown at the bottom of this page.*

Proof: See Appendix A. □

B. SCHEME 2

1) OUTAGE PROBABILITY OF D_1

Here, we explore the situation where D_1 harvests energy from the RF signal that is sent from the BS. Following the same approach as in Scheme 1, the outage probability of D_1 is formulated as

$$OP_{1-NOMA}^{FD-EH} = 1 - \Pr\left(\gamma_{SD1\leftarrow 2}^{NOMA-EH} \geqslant \varepsilon_2^{FD}, \gamma_{SD1}^{NOMA-EH} \geqslant \varepsilon_1^{FD}\right). \quad (36)$$

Theorem 3: The closed-form expression for the outage probability at D_1 in this scheme is given in (37) *at the bottom of the next page.*

2) OUTAGE PROBABILITY OF D_2

Based on (34), the outage probability of D_2 in this case is formulated as

$$\begin{aligned} OP_{2-NOMA}^{FD-EH} &= \Pr\left[\max\left(\min\left(\gamma_{SD1\leftarrow 2}^{NOMA-EH}, \gamma_{D12,x2}^{NOMA-EH}\right), \max_{k=1,\cdots,K} \min\left(\gamma_{SRK,x2}^{NOMA}, \gamma_{RKD2,x2}^{NOMA}\right)\right) < \varepsilon_2^{FD}\right] \\ &= \Pr\left[\min\left(\gamma_{SD1\leftarrow 2}^{NOMA-EH}, \gamma_{D12,x2}^{NOMA-EH}\right) < \varepsilon_2^{FD}, \max_{k=1,\cdots,K} \min\left(\gamma_{SRK,x2}^{NOMA}, \gamma_{RKD2,x2}^{NOMA}\right) < \varepsilon_2^{FD}\right]. \end{aligned} \quad (38)$$

Theorem 4: For Scheme 2, the outage probability of D_2 is obtained in (39) *and it is displayed at the bottom of the next page.*

Proof: See Appendix B. □

C. SCHEME 3

In this subsection, we investigate the outage probability of D_1 and D_2 for the cases of QMFR with energy harvesting at D_1 (QMFR EH) and without energy harvesting at D_1 (QMFR Non-EH), respectively.

1) OUTAGE PROBABILITY OF D_1

In this scheme, an outage event occurs at D_1 if it cannot detect its own signal. Therefore, the outage probability of D_1 in the case of QMFR Non-EH and QMFR EH are given by

$$OP_{1-NOMA}^{FD-QMF} = 1 - \Pr\left(\gamma_{SD1}^{QMF} \geq \varepsilon_1^{FD}\right), \quad (40)$$

and

$$OP_{1-NOMA}^{FD-QMF-EH} = 1 - \Pr\left(\gamma_{SD1}^{QMF-EH} \geq \varepsilon_1^{FD}\right), \quad (41)$$

respectively.

Theorem 5: For QMFR Non-EH and QMFR EH, the outage probability of D_1 can be obtained as (42) *and* (43), *respectively, which is valid for $a_1 > \varepsilon_1^{FD} a_2$, otherwise D_1 is always in outage.*

Proof: See Appendix C. □

2) OUTAGE PROBABILITY OF D_2

Similarly, we evaluate the outage probability of D_2 with and without energy harvesting at D_1.

In case D_1 is not energy harvesting, the outage probability at D_2 can be formulated as

$$\begin{aligned} OP_{2-NOMA}^{FD-QMF} = &\left[1 - \Pr\left(\gamma_{SD1}^{QMF} \geq \varepsilon_1^{FD}, \gamma_{SD1,x2}^{QMF} \geq \varepsilon_2^{FD}, \gamma_{D12,x2}^{NOMA} \geq \varepsilon_2^{FD}\right)\right] \\ &\times \prod_{k=1}^{K}\left[1 - \Pr\left(\gamma_{SRK,x1}^{QMF} \geq \varepsilon_1^{FD}, \gamma_{SRK,x2}^{QMF} \geq \varepsilon_2^{FD}, \gamma_{RKD2,x2}^{NOMA} \geq \varepsilon_2^{FD}\right)\right]. \end{aligned} \quad (44)$$

Theorem 6: The outage probability of D_2 in case of QMFR Non-EH is evaluated as

$$\begin{aligned} OP_{2-NOMA}^{FD-QMF} = &\left[1 - \sum_{n=1}^{N}\binom{N}{n}(-1)^{n-1} \times \frac{\lambda_{g1,n}}{n\theta\omega\rho\lambda_{hD1} + \lambda_{g1,n}} \exp\left(-\frac{n\theta}{\lambda_{g1,n}} - \frac{\varepsilon_2^{FD}}{\rho\lambda_{h1}}\right)\right] \\ &\times \prod_{k=1}^{K}\left[1 - \sum_{n=1}^{N}\binom{N}{n}(-1)^{n-1} \times \frac{\lambda_{gn,k}}{n\theta\omega\rho\lambda_{hr_k} + \lambda_{gn,k}} \exp\left(-\frac{n\theta}{\lambda_{gn,k}} - \frac{\varepsilon_2^{FD}}{\rho\lambda_{h2}}\right)\right], \end{aligned} \quad (45)$$

which is valid for $a_1 > \varepsilon_1^{FD} a_2$ and

$$\theta = \max\left(\frac{\varepsilon_1^{FD}}{a_1\rho - \varepsilon_1^{FD} a_2\rho}, \frac{\varepsilon_2^{FD}}{a_2\rho}\right).$$

Proof: See Appendix D. □

Besides, the outage probability of D_2 in the case of energy harvesting at D_1, i.e., QMFR EH scenario, is formulated as

$$OP_{2-NOMA}^{FD-QMF-EH} = \left[1 - \Pr\left(\gamma_{SD1}^{QMF-EH} \geq \varepsilon_1^{FD},\right.\right.$$

$$\begin{aligned} OP_{2-NOMA}^{FD} = &\left[1 - \sum_{n=1}^{N}\binom{N}{n}(-1)^{n-1} \frac{\left(a_2\rho - \varepsilon_2^{FD} a_1\rho\right)\lambda_{g1,n}}{n\varepsilon_2^{FD}\omega\rho\lambda_{D1} + \left(a_2\rho - \varepsilon_2^{FD} a_1\rho\right)\lambda_{g1,n}} \exp\left(-\frac{n\varepsilon_2^{FD}}{\left(a_2\rho - \varepsilon_2^{FD} a_1\rho\right)\lambda_{g1,n}} - \frac{\varepsilon_2^{FD}}{\rho\lambda_{h1}}\right)\right] \\ &\times \prod_{k=1}^{K}\left(1 - \sum_{n=1}^{N}\binom{N}{n}(-1)^{n-1} \frac{\left(a_2 - \varepsilon_2^{FD} a_1\right)\rho\lambda_{gn,k}}{n\varepsilon_2^{FD}\omega\rho\lambda_{hr_k} + \left(a_2 - \varepsilon_2^{FD} a_1\right)\rho\lambda_{gn,k}} \exp\left(-\frac{n\varepsilon_2^{FD}}{\left(a_2 - \varepsilon_2^{FD} a_1\right)\rho\lambda_{gn,k}} - \frac{\varepsilon_2^{FD}}{\rho\lambda_{h2}}\right)\right) \end{aligned} \quad (35)$$

$$\left.\left.\gamma_{SD1,x2}^{QMF-EH} \geq \varepsilon_2^{FD}, \gamma_{D12,x2}^{NOMA-EH} \geq \varepsilon_2^{FD}\right)\right] \times \prod_{k=1}^{K}\left[1 - \Pr\left(\gamma_{SRK,x1}^{QMF} \geq \varepsilon_1^{FD},\right.\right. \left.\left.\gamma_{SRK,x2}^{QMF} \geq \varepsilon_2^{FD}, \gamma_{RKD2,x2}^{NOMA} \geq \varepsilon_2^{FD}\right)\right]. \quad (46)$$

Theorem 7: For QMFR EH, the outage probability of D_2 is obtained in (47)*, shown at the bottom of the next page, where* $\zeta = \max\left(\frac{\varepsilon_1^{FD}}{(1-\beta)(a_1\rho-\varepsilon_1^{FD}a_2\rho)}, \frac{\varepsilon_2^{FD}}{(1-\beta)a_2\rho}\right)$ *and the condition of* $a_1 > \varepsilon_1^{FD}a_2$ *must be guaranteed.*

Proof: See Appendix E. □

It is noted that the outage probability for the three schemes assuming HD mode can be obtained by setting $\omega = 0$ and replacing $\varepsilon_i^{FD} = 2^{R_i} - 1$ by $\varepsilon_i^{HD} = 2^{2R_i} - 1, (i = 1, 2)$, in the corresponding FD outage probability expressions.

Corollary: From the outage probability expressions derived above, the system throughput of the aforementioned FD and HD NOMA scenario for each scheme is obtained as

$$\Gamma_v^u = \left(1 - OP_{1-NOMA}^u\right) R_1 + \left(1 - OP_{2-NOMA}^u\right) R_2, \quad (48)$$

where $v = (1, 2, 3)$ denotes Scheme 1, scheme 2 and scheme 3, respectively and $u = \{FD, HD, FD\_EH, HD\_EH, FD\_QMF, HD\_QMF, FD\_QMF\_EH, HD\_QMF\_EH\}$ denotes the considered protocol in the three schemes.

IV. NUMERICAL RESULTS

In this section, we examine the accuracy of the derived analytical results and assess the performance of the considered system by Monte Carlo simulations. Without loss of generality, we assume that the power allocation coefficients of NOMA are $a_1 = 0.3$ and $a_2 = 0.7$ for D_1 and D_2, respectively. In addition, it is assumed that the distance between the devices in the system normalized to one. In this context, unless otherwise stated, the solid lines denote the derived analytical results while the respective Monte-Carlo simulation results are presented using the markers. Thus, it can be observed that the analytical curves perfectly match the corresponding simulation results which demonstrates the accuracy of derived analytical expressions. We call bit per channel user in short as BPCU.

$$\begin{aligned} OP_{1-NOMA}^{FD-EH} &= 1 - \int_0^\infty \left(1 - F_{|g_{1,n^*}|^2}\left(\frac{(\omega\rho x + 1)}{(1-\beta)}\psi_1\right)\right) f_{|h_{D1}|^2}(x)\, dx \\ &= 1 - \int_0^\infty \sum_{n=1}^{N}\binom{N}{n}(-1)^{n-1}\exp\left(-\frac{n(\omega\rho x + 1)\psi_1}{(1-\beta)\lambda_{g1,n}}\right)\frac{1}{\lambda_{hD1}}\exp\left(-\frac{x}{\lambda_{hD1}}\right)dx \\ &= 1 - \sum_{n=1}^{N}\binom{N}{n}(-1)^{n-1}\frac{1}{\lambda_{hD1}}\exp\left(-\frac{n\psi_1}{(1-\beta)\lambda_{g1,n}}\right)\int_0^\infty \exp\left(-\left(\frac{n\omega\rho\psi_1}{(1-\beta)\lambda_{g1,n}} + \frac{1}{\lambda_{hD1}}\right)x\right)dx \\ &= 1 - \sum_{n=1}^{N}\binom{N}{n}(-1)^{n-1}\frac{(1-\beta)\lambda_{g1,n}}{n\omega\rho\psi_1\lambda_{hD1} + (1-\beta)\lambda_{g1,n}}\exp\left(-\frac{n\psi_1}{(1-\beta)\lambda_{g1,n}}\right) \end{aligned} \quad (37)$$

$$\begin{aligned} OP_{2-NOMA}^{FD-EH} = &\left[1 - \sum_{n=1}^{N}\binom{K}{n}(-1)^{n-1}\frac{(1-\beta)\left(a_2 - a_1\varepsilon_2^{FD}\right)\rho\lambda_{1,n}}{n\varepsilon_2^{FD}\omega\rho\lambda_{D1} + (1-\beta)\left(a_2 - a_1\varepsilon_2^{FD}\right)\rho\lambda_{1,n}}\exp\left(-\frac{n\varepsilon_2^{FD}}{(1-\beta)\left(a_2 - a_1\varepsilon_2^{FD}\right)\rho\lambda_{1,n}}\right)\right. \\ &\times \sum_{n=1}^{N}\binom{N}{n}(-1)^{n-1} \\ &\times \left.\frac{1}{\lambda_{h1}}\int_0^\infty \frac{\rho y\lambda_{g1,n}}{n\varepsilon_2^{FD}\lambda_{D1} + \rho y\lambda_{g1,n}}\left[\exp\left(-\left(\frac{1}{\beta}-1\right)\frac{n\varepsilon_2^{FD}}{\eta\rho y\lambda_{g1,n}} - \frac{y}{\lambda_{h1}} - \frac{1}{\eta\lambda_{D1}}\right) - \exp\left(-\frac{n\varepsilon_2^{FD}}{\eta\beta\rho y\lambda_{g1,n}} - \frac{y}{\lambda_{h1}}\right)\right]dy\right] \\ &\times \prod_{k=1}^{K}\left(1 - \sum_{n=1}^{N}\binom{N}{n}(-1)^{n-1}\frac{\left(a_2 - \varepsilon_2^{FD}a_1\right)\rho\lambda_{gn,k}}{n\varepsilon_2^{FD}\omega\rho\lambda_{hr_k} + \left(a_2 - \varepsilon_2^{FD}a_1\right)\rho\lambda_{gn,k}}\exp\left(-\frac{n\varepsilon_2^{FD}}{\left(a_2 - \varepsilon_2^{FD}a_1\right)\rho\lambda_{gn,k}} - \frac{\varepsilon_2^{FD}}{\rho\lambda_{h2}}\right)\right) \end{aligned} \quad (39)$$

$$OP_{1-NOMA}^{FD-QMF} = 1 - \sum_{n=1}^{N}\binom{N}{n}(-1)^{n-1}\frac{\left(a_1 - \varepsilon_1^{FD}a_2\right)\rho\lambda_{g1,n}}{n\varepsilon_1^{FD}\omega\rho\lambda_{hD1} + \left(a_1 - \varepsilon_1^{FD}a_2\right)\rho\lambda_{g1,n}}\exp\left(-\frac{n\varepsilon_1^{FD}}{\left(a_1 - \varepsilon_1^{FD}a_2\right)\rho\lambda_{g1,n}}\right). \quad (42)$$

$$OP_{1-NOMA}^{FD-QMF-EH} = 1 - \sum_{n=1}^{N}\binom{N}{n}(-1)^{n-1}\frac{(1-\beta)\left(a_1 - \varepsilon_1^{FD}a_2\right)\rho\lambda_{g1,n}}{n\varepsilon_1^{FD}\omega\rho\lambda_{hD1} + (1-\beta)\left(a_1 - \varepsilon_1^{FD}a_2\right)\rho\lambda_{g1,n}}\exp\left(-\frac{n\varepsilon_1^{FD}}{(1-\beta)\left(a_1 - \varepsilon_1^{FD}a_2\right)\rho\lambda_{g1,n}}\right) \quad (43)$$

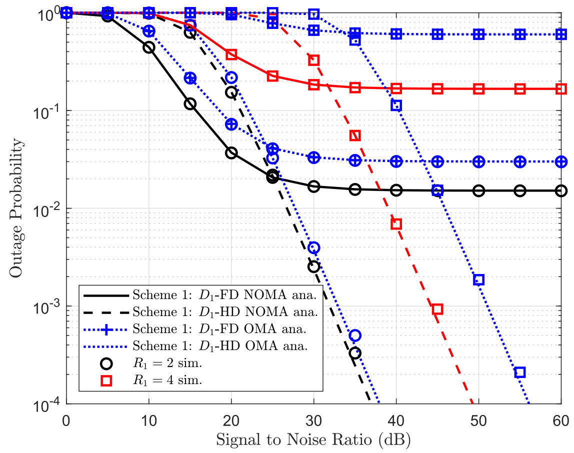

FIGURE 2. **Outage probability of D_1 versus SNR for different values of R_1 when $\lambda_{g1,n} = 1$, $\lambda_{hD1} = 0.01$, $N = 2$.**

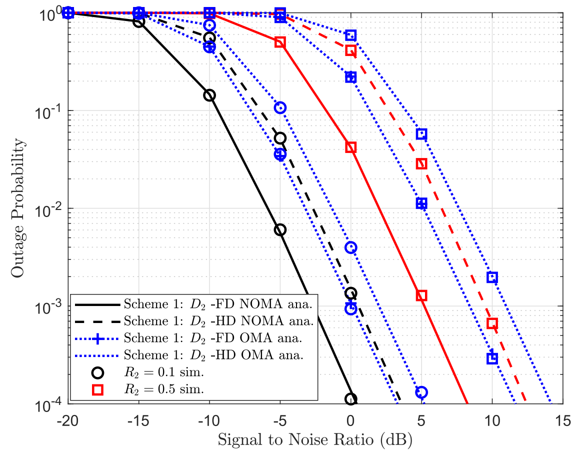

FIGURE 3. **Outage probability of D_2 versus SNR for different values of R_2 when $\lambda_{g1,n} = 1$, $\lambda_{gn,k} = 5$, $\lambda_{h1} = 4$, $\lambda_{h2} = 1$, $\lambda_{hD1} = \lambda_{hr_k} = 0.01$, and $K = N = 2$.**

A. SCHEME 1: NON ENERGY HARVESTING - NON-EHR

This subsection examines the system's outage probability when there is no energy harvesting at D_1. To this end, Fig. 2 shows the outage probability versus SNR which are achieved from the expression (28), (29) and HD mode, respectively. It can be seen that the performance of FD NOMA is better than HD NOMA at low SNR, i.e., SNR from $10\,dB$ to $25\,dB$, but the performance of the HD NOMA mode is superior in the high SNR region ($SNR \geqslant 30\,dB$). This is because as the SNR increases, the FD mode is strongly influenced by self-interference which consequently decreases the performance.

Furthermore, in Fig. 2, it is shown that the NOMA technique outperforms the conventional OMA technology where the signal transmission is performed in three time slots, i.e., the BS sends the signal x_1 to D_1 in the first time slot and x_2 to D_2 in the second time slot, while in the last time slot, D_1 decodes and forwards the signal x_2 to D_2.

The outage performance of D_2 is shown in Fig. 3, where it is clearly observed that the outage performance of the FD NOMA mode is superior to both the HD NOMA and the OMA mode. Moreover, looking at Fig. 4, it's also noticed that when increasing the number of relay nodes, the performance is also improved, since increasing the relay nodes will improve the channel diversity gain. In other words, an outage event will be more difficult to happen.

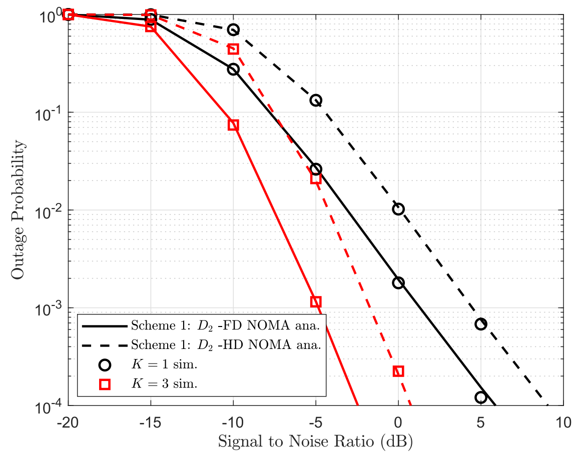

FIGURE 4. **Outage probability of D_2 versus SNR for different numbers of relay nodes in the system (K) with $\lambda_{g1,n} = 1$, $\lambda_{gn,k} = 5$, $\lambda_{h1} = 4$, $\lambda_{h2} = 1$, $\lambda_{hD1} = \lambda_{hr_k} = 0.01$, $N = 2$, and $R_2 = 0.1$ (BPCU).**

$$
\begin{aligned}
OP_{2-NOMA}^{FD-QMF-EH} &= \left[1 - \sum_{n=1}^{N} \binom{N}{n} (-1)^{n-1} \frac{\lambda_{g1,n}}{n\zeta\omega\rho\lambda_{hD1} + \lambda_{g1,n}} \exp\left(-\frac{n\zeta}{\lambda_{g1,n}}\right)\right. \\
&\times \sum_{n=1}^{N} \binom{N}{n} (-1)^{n-1} \frac{1}{\lambda_{h1}} \\
&\times \int_0^{\infty} \frac{\rho y \lambda_{g1,n}}{n\varepsilon_2^{FD}\lambda_{D1} + \rho y \lambda_{g1,n}} \left[\exp\left(-\left(\frac{1}{\beta}-1\right)\frac{n\varepsilon_2^{FD}}{\eta\rho y\lambda_{g1,n}} - \frac{y}{\lambda_{h1}} - \frac{1}{\eta\lambda_{D1}}\right) - \exp\left(-\frac{n\varepsilon_2^{FD}}{\eta\beta\rho y\lambda_{g1,n}} - \frac{y}{\lambda_{h1}}\right)\right] dy \\
&\times \prod_{k=1}^{K} \left[1 - \exp\left(-\frac{\varepsilon_2^{FD}}{\rho\lambda_{h2}}\right) \times \sum_{n=1}^{N} \binom{N}{n} (-1)^{n-1} \frac{\lambda_{gn,k}}{n\theta\omega\rho\lambda_{hr_k} + \lambda_{gn,k}} \exp\left(-\frac{n\theta}{\lambda_{gn,k}}\right)\right]
\end{aligned} \tag{47}
$$

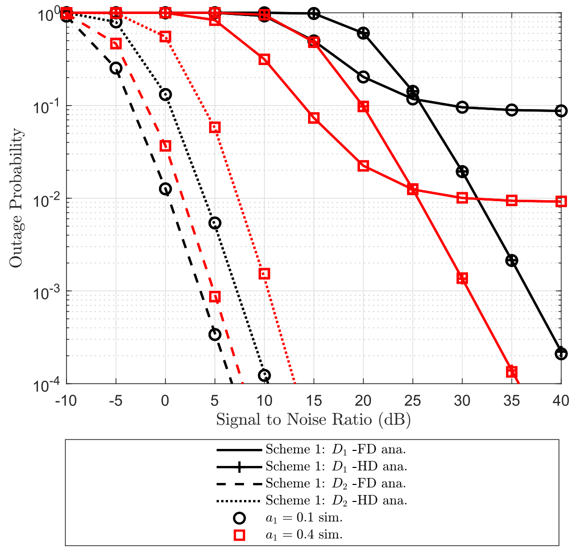

FIGURE 5. Comparison of the outage probability of D_1 and D_2 for various power allocation coefficients when $\lambda_{g1,n} = 1$, $\lambda_{gn,k} = 5$, $\lambda_{h1} = 4$, $\lambda_{h2} = 1$, $\lambda_{hD1} = \lambda_{hr_k} = 0.01$, $N = 2$, $R_1 = 2$ (BPCU), $R_2 = 0.4$ (BPCU), and $N = K = 2$.

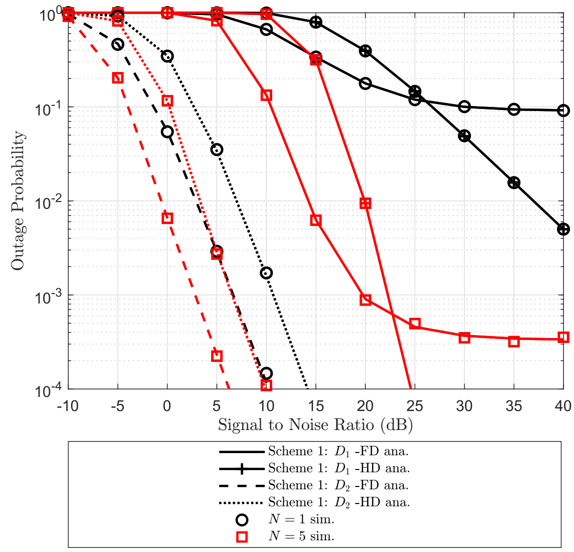

FIGURE 6. Outage probability of D_1 and D_2 for different numbers of BS antennas when $\lambda_{g1,n} = 1$, $\lambda_{gn,k} = 5$, $\lambda_{h1} = 4$, $\lambda_{h2} = 1$, $\lambda_{hD1} = \lambda_{hr_k} = 0.01$, $N = 2$, $R_1 = 2$ BPCU, $R_2 = 0.4$ BPCU, and $K = 2$.

In Fig. 5, the comparison of the outage performance between D_1 and D_2 in both HD NOMA and FD NOMA with different power allocation coefficients has been expressed. There is a large outage performance gap between D_1 and D_2 when the SNR increases from 25 (dB) to 40 (dB). In addition, it can be recognized that the outage probability curves of D_2 are almost unchanged a lot when changing the value of a_1. However, it has great impact on the outage probability of D_1. This implies that there should be a reasonable strategy in selecting the power allocation coefficients when deploying real network in the future.

The influence of the number of antennas at the BS on the outage performance of the system is clearly shown in Fig. 6. We can see that the system's outage performance follows the same trend for the different numbers of antennas considered; however, increasing the number of antennas greatly improves the outage performance, especially for Scheme 1.

In Fig. 7, we plot and compare the throughput of the FD NOMA and HD NOMA cases obtained in (48). The black solid curves and the red solid curve denote the FD and HD NOMA cases, respectively, while the dashed curves represent the OMA scheme. It is observed that the FD NOMA system throughput is superior to the HD NOMA and OMA cases, especially in the low SNR region and for low SI values while higher SI values significantly affect the performance of FD NOMA, making it perform the worst among the 3 considered scenarios.

B. SCHEME 2: ENERGY HARVESTING- EHR

In this subsection, the outage performance of D_1 and D_2 is for the energy harvesting case.

Fig. 8 and Fig. 9 show the FD and HD modes outage performance of D_1 and D_2 with various target rates, respectively.

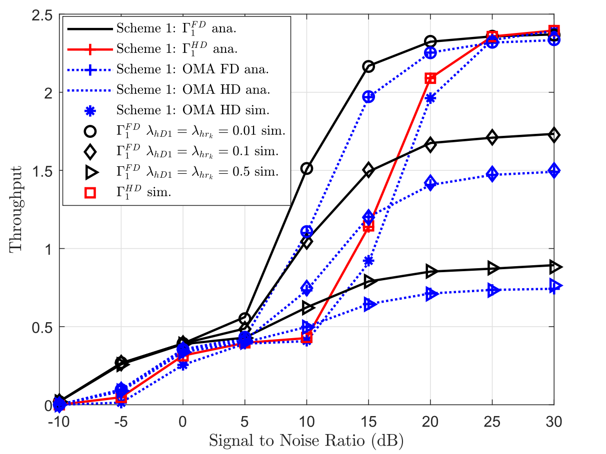

FIGURE 7. System throughput of Scheme 1 for different values of SI when $\lambda_{g1,n} = 1$, $\lambda_{gn,k} = 5$, $\lambda_{h1} = 4$, $\lambda_{h2} = 1$, $\lambda_{hD1} = \lambda_{hr_k} = 0.01$, $R_1 = 2$ BPCU, $R_2 = 0.4$ BPCU, and $N = K = 2$.

Similarly to the Scheme 1 case, the outage performance of D_1 and D_2 in FD mode is better than HD mode where, generally the performance of NOMA surpasses that of the conventional the OMA scheme. Besides, when the objective rate is reduced, the outage performance of the two users is also improved.

Fig. 10 compares the outage probabilities of D_1 and D_2 in HD and FD mode. It can be seen that the outage performance of D_1 in FD mode is better than HD mode when the SNR is between 0 dB and 25 dB. In addition, when increasing the power allocation factor of D_1, i.e., a_1, the outage performance of D_1 is improved. For D_2, the outage performance in FD mode is always better than HD mode. However, it is noted that according to the NOMA principle, when increasing a_1, this means reducing a_2. Hence, the outage performance of D_2

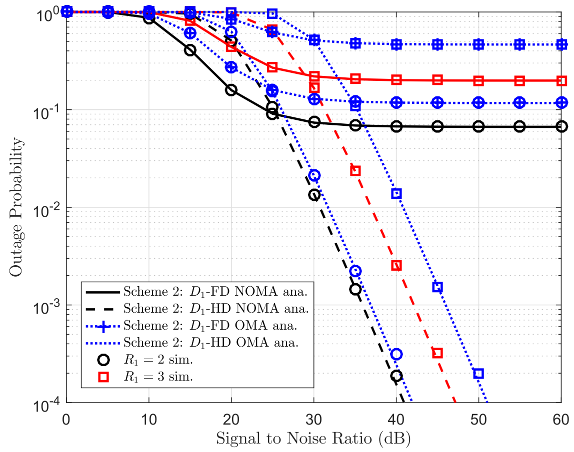

FIGURE 8. Outage probability of D_1 versus SNR for different values of R_1 when $\lambda_{g1,n} = 1$, $\lambda_{hD1} = 0.01$, $\eta = \beta = 0.6$, and $N = 2$.

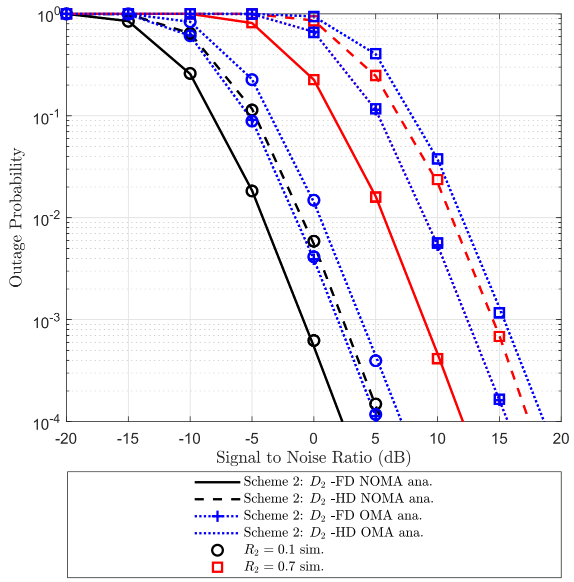

FIGURE 9. Outage probability of D_2 versus SNR for different values of R_2 when $\lambda_{g1,n} = 1$, $\lambda_{gn,k} = 5$, $\lambda_{h1} = 4$, $\lambda_{h2} = 1$, $\lambda_{hD1} = \lambda_{hr_k} = 0.01$, $R_1 = 2$ BPCU, $R_2 = 0.4$ BPCU, and $N = K = 2$.

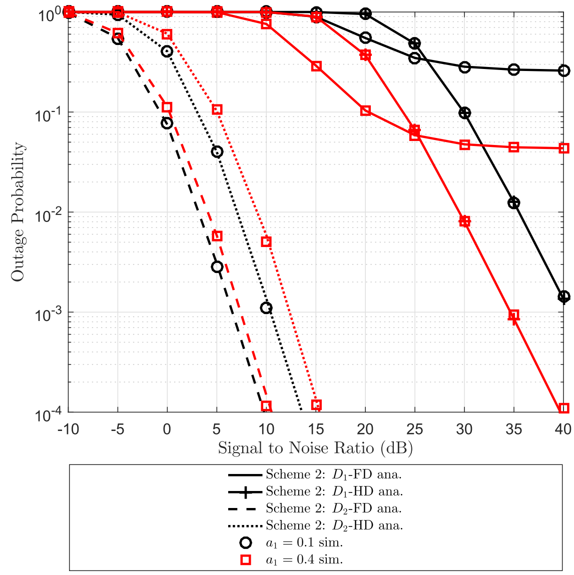

FIGURE 10. Outage probability of D_1 and D_2 for different power allocation coefficients a_1 when $\lambda_{g1,n} = 1$, $\lambda_{gn,k} = 5$, $\lambda_{h1} = 4$, $\lambda_{h2} = 1$, $\lambda_{hD1} = \lambda_{hr_k} = 0.01$, $R_1 = 2$ BPCU, $R_2 = 0.5$ BPCU, $\eta = \beta = 0.6$, and $N = K = 2$.

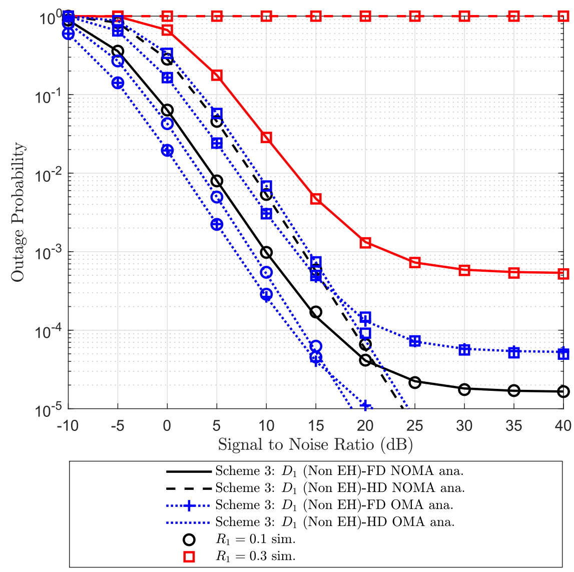

FIGURE 11. Outage probability of D_1 for the QMFR Non-EH versus SNR for different values of R_1 when $\lambda_{g1,n} = 1$, $\lambda_{hD1} = 0.01$, and $N = 2$.

is decreased. Moreover, it can be observed from Fig. 10 that the outage performance of D_2 is superior to D_1 and the higher the SNR, the more obvious the superiority is.

C. SCHEME 3: QMF RELAYING - QMFR

In this subsection, the outage performance for the case of QMFR EH and QMFR Non-EH in FD and HD mode is verified. In particular, the outage performance of D_1 and D_2 in both cases, with and without energy harvesting are considered.

The outage probability of D_1 in the QMFR Non-EH and QMFR EH are shown in Fig. 11 and Fig. 12, respectively. It can be seen that the FD mode achieves higher performance than the HD mode in the SNR region from 0 to 20 dB. Especially, when increasing $R_1 = 0.3$ PBCU, there is an outage event that occurs in HD mode while the outage performance of FD mode is still guaranteed. The reason behind this is that when $a_1 = 0.3$ and $R_1 = 0.3$ PBCU, the condition in (40), i.e., $a_1 > \varepsilon_1^{FD} a_2$ is guaranteed for the FD mode, but the condition for HD mode, i.e., $a_1 > \varepsilon_1^{HD} a_2$ is no longer guaranteed, so the outage probability in HD mode will be one. Besides, one can see from Fig. 11 and Fig. 12 that the outage probability of D_1 is affected by the energy harvesting. This proves that the outage probability of D_1 in this Scheme is not greatly influenced by the energy harvesting process. Additionally, it is noticed that OMA has a better out-

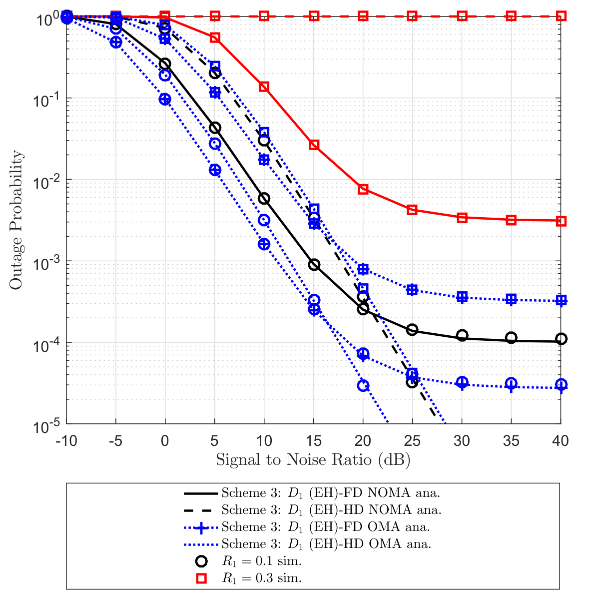

FIGURE 12. Outage probability of D_1 for the QMFR EH versus SNR for different values of R_1 when $\lambda_{g1,n} = 1$, $\lambda_{hD1} = 0.01$, $\beta = 0.6$, and $N = 2$.

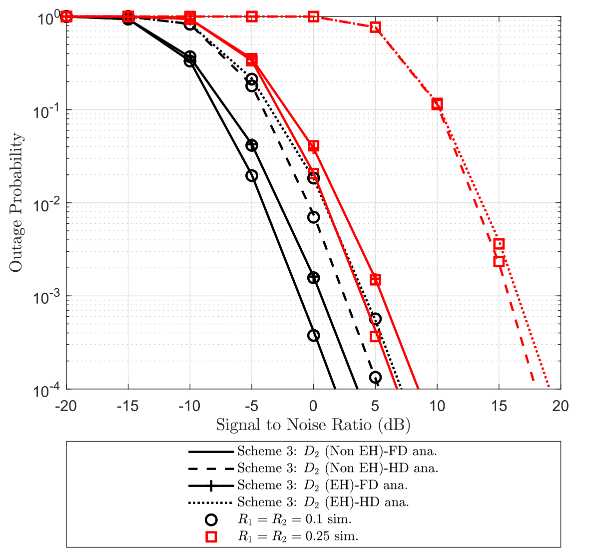

FIGURE 13. Outage probability of D_2 in the case of QMFR EH and QMFR Non-EH protocol with different values of R_1 and R_2 when $\lambda_{g1,n} = 1$, $\lambda_{gn,k} = 5$, $\lambda_{h1} = 4$, $\lambda_{h2} = 1$, $\lambda_{hD1} = \lambda_{hr_k} = 0.01$, $\eta = \beta = 0.6$, and $N = K = 2$.

age performance than NOMA. This is in line with the QMF protocol, where D_1 prioritizes decoding its signal first, and considers D_2's signal as interference, leading to a decrease in the outage performance of D_1.

Fig. 13 shows the outage probability of D_2 for different values of R_1 and R_2. It is noted that when $a_1 = 0.3$, the value of R_1 must be less than 0.5 for FD and less than 0.25 for HD mode in order to ensure that the conditions $a_1 > \varepsilon_1^{FD} a_2$ and $a_1 > \varepsilon_1^{HD} a_2$ are satisfied. It can be noticed that the outage performance of FD mode is always better than the HD mode for both the case of QMFR EH and QMFR Non- EH

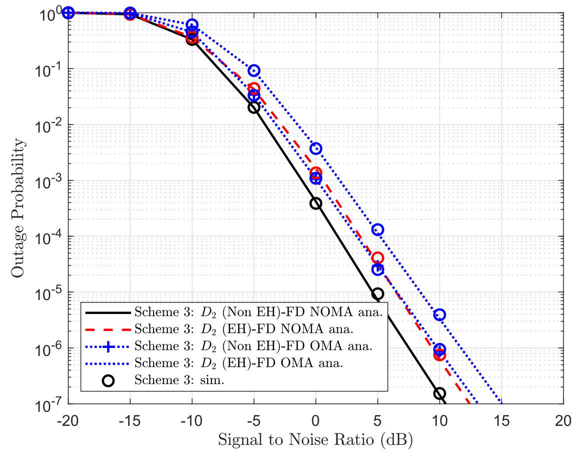

FIGURE 14. Outage probability of D_2 in the case of QMFR EH and QMFR Non-EH protocol compared with OMA scheme when system in FD mode and $\lambda_{g1,n} = 1$, $\lambda_{gn,k} = 5$, $\lambda_{h1} = 4$, $\lambda_{h2} = 1$, $\lambda_{hD1} = \lambda_{hr_k} = 0.01$, $\eta = \beta = 0.6$, $R_1 = R_2 = 0.1$ BPCU, and $N = K = 2$.

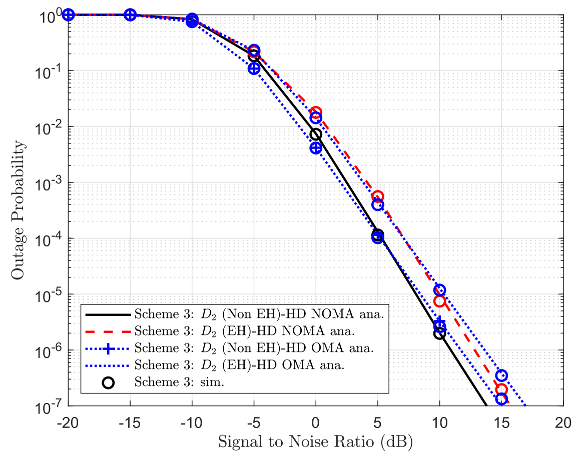

FIGURE 15. Outage probability of D_2 in the case of QMFR EH and QMFR Non-EH protocol compared with OMA scheme when system in HD mode and $\lambda_{g1,n} = 1$, $\lambda_{gn,k} = 5$, $\lambda_{h1} = 4$, $\lambda_{h2} = 1$, $\lambda_{hD1} = \lambda_{hr_k} = 0.01$, $\eta = \beta = 0.6$, $R_1 = R_2 = 0.1$ BPCU, and $N = K = 2$.

protocol. In addition, when the target rate is increased from 0.1 to 0.25 BPCU, the QMFR Non-EH achieves relatively better outage performance than the QMFR EH. Besides, when increasing R_1 and R_2, i.e., $R_1 = R_2 = 0.25$ BPCU, there is a big gap between FD and HD mode. In other words, the superiority of FD mode over HD is more evident when the target rate is increased.

The outage performance of D_2 with both NOMA and OMA schemes are shown in Fig. 14 and Fig. 15 for the FD and HD modes, respectively. It can be seen from Fig. 14 that the QMFR EH and QMFR Non-EH protocols have a lower outage probability than OMA in FD mode. However, for HD mode, which is shown in Fig. 15, the outage performance of OMA is slightly better than the QMFR EH and QMFR Non-EH protocols in the low SNR region and vice versa in the high SNR area. The reason for this is that D_1 may be in outage

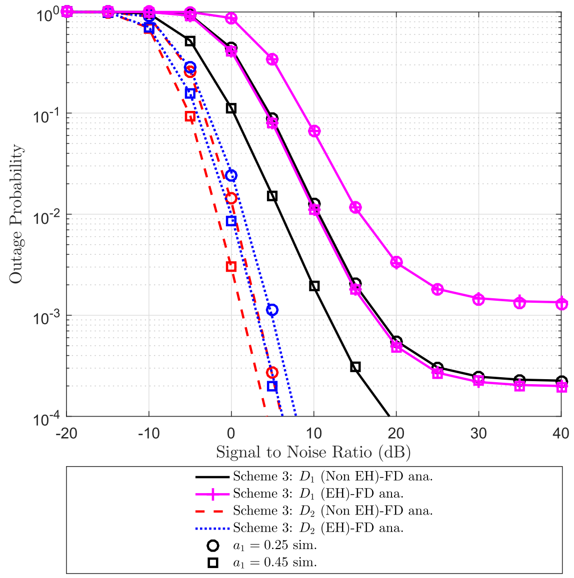

FIGURE 16. **Outage probability of D_1 and D_2 assuming different power allocation coefficients a_1 for $\lambda_{g1,n} = 1$, $\lambda_{gn,k} = 5$, $\lambda_{h1} = 4$, $\lambda_{h2} = 1$, $\lambda_{hD1} = \lambda_{hr_k} = 0.01$, $\eta = \beta = 0.6$, and $N = K = 2$.**

state or unable to decode its own signal in the low SNR area. Consequently, D_1 cannot forward information to D_2.

Fig. 16 shows the outage probability of both D_1 and D_2 in FD mode. The solid lines in black and purple depict the outage probability of D_1 in QMFR Non-EH and QMFR EH, respectively, while the dashed lines in red and blue show the corresponding outage probability of D_2. It can be observed that, when a_1 increases, the outage probability is reduced. In other words, the outage performance increases. Specially, in contrast to schemes 1 and 2, when a_1 increases, the outage performance of D_2 improves. This can be explained by the fact that there are differences in the conditions in (45) and (47), i.e., $a_1 > \varepsilon_1^{FD} a_2$, and this means increasing a_1, increases the chances of satisfying this condition which increases the outage performance of D_2. In addition, we also find from Fig. 16 that the outage performance of D_2 in QMFR EH is lower than D_2 in the QMFR Non-EH protocol when the SNR increases.

Fig. 17 plots the outage probability of D_2 in EH mode and compares between schemes 2 and 3. Here, it is demonstrated that the outage performance is improved when the energy conversion factor is increased. Moreover, for D_2, scheme 2 achieves better performance than scheme 3.

Fig. 18 compares the outage probability of D_2 in Scheme 1, scheme 2 and scheme 3 to each other when changing the number of relay nodes. Besides, the impact of the number of relay nodes on the outage performance of D_2 is also considered. For simplicity, Fig. 18 shows only the FD mode. The simulation and analysis results have demonstrated that the outage performance is significantly improved when the number of relay increases. Moreover, it is also shown that Scheme 1 achieves the best outage performance.

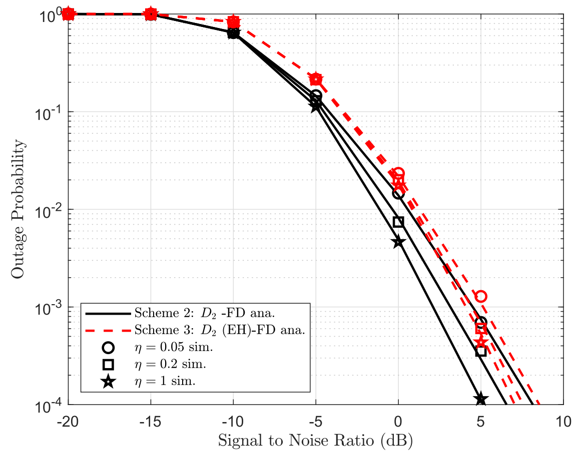

FIGURE 17. **Outage probability of D_2 for Schemes 2 and 3 for various energy conversion coefficients when $\lambda_{g1,n} = 1$, $\lambda_{gn,k} = 5$, $\lambda_{h1} = 4$, $\lambda_{h2} = 1$, $\lambda_{hD1} = \lambda_{hr_k} = 0.01$, $R_1 = R_2 = 0.2$ BPCU, $\beta = 0.6$, and $N = K = 2$.**

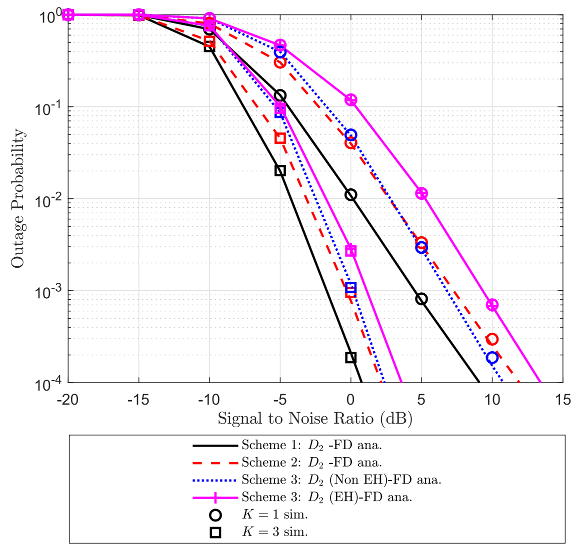

FIGURE 18. **Outage probability of D_2 versus SNR for schemes 1, 2 and 3 with different number of relay nodes when $\lambda_{g1,n} = 1$, $\lambda_{gn,k} = 5$, $\lambda_{h1} = 4$, $\lambda_{h2} = 1$, $\lambda_{hD1} = \lambda_{hr_k} = 0.01$, $R_1 = R_2 = 0.2$ BPCU, $\beta = \eta = 0.6$, and $N = K = 2$.**

The general comparison between the outage performance of the three schemes is shown in Fig. 19 and Fig. 20 for the FD and HD modes, respectively where it s shown that Scheme 1 has a superior performance compared to the other schemes.

Fig. 21 shows the outage probability of the three schemes in FD mode versus the power allocation coefficient a_1. As mentioned above, the condition for the outage performance is guaranteed to be $a_2 > \varepsilon_2^{FD} a_1$ for schemes 1 and 2, while for scheme 3, it is $a_1 > \varepsilon_1^{FD} a_2$. Therefore, when $R_1 = R_2 = 0.4$ BPCU, the condition becomes $a_2 > 0.3\, a_1$ for schemes 1 and 2, and $a_1 > 0.3\, a_2$ for scheme 3. It can be observed from Fig. 21 that schemes 1 and 2 will be in outage when $a_1 \geq 0.7$ while scheme 3 is in outage when

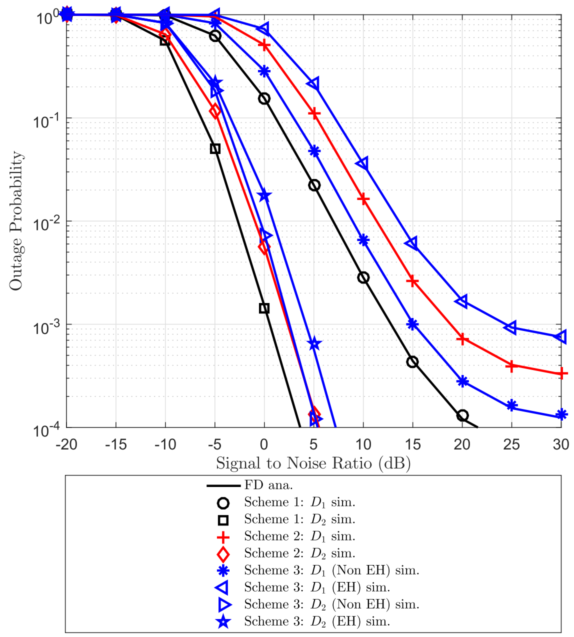

FIGURE 19. Comparison between the outage probability of the three schemes in FD mode when $\lambda_{g1,n} = 1$, $\lambda_{gn,k} = 5$, $\lambda_{h1} = 4$, $\lambda_{h2} = 1$, $\lambda_{hD1} = \lambda_{hr_k} = 0.01$, $R_1 = R_2 = 0.2$ BPCU, $\beta = \eta = 0.6$, and $N = K = 2$.

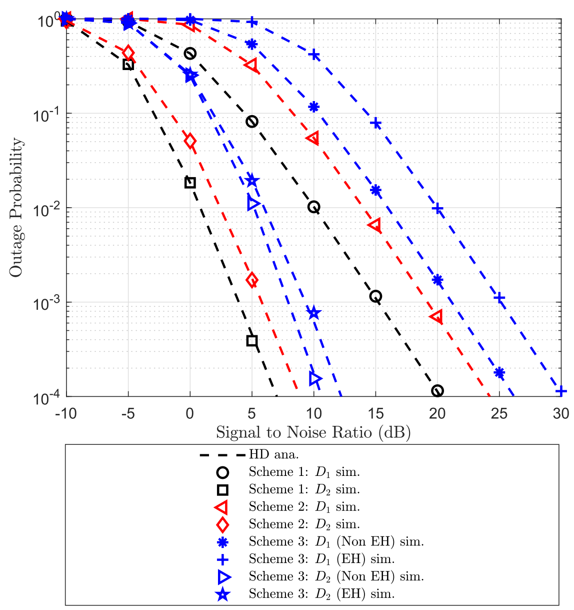

FIGURE 20. Comparison between the outage probability of the three schemes in HD mode when $\lambda_{g1,n} = 1$, $\lambda_{gn,k} = 5$, $\lambda_{h1} = 4$, $\lambda_{h2} = 1$, $\lambda_{hD1} = \lambda_{hr_k} = 0.01$, $R_1 = R_2 = 0.2$ BPCU, $\beta = \eta = 0.6$, and $N = K = 2$.

$a_1 \leq 0.3$ or $a_1 = 1$, this is completely consistent with the conditions analyzed. In addition, the optimal power allocation coefficient for the three schemes can be determined. Specifically, the optimal values of a_1 for schemes 1, 2, and 3 are 0.1, 0.2 and 0.5, respectively.

Fig. 22 compares the throughput of all three schemes when $a_1 = 0.3$ and $R_1 = R_2 = 0.2$ BPCU in order to ensure that

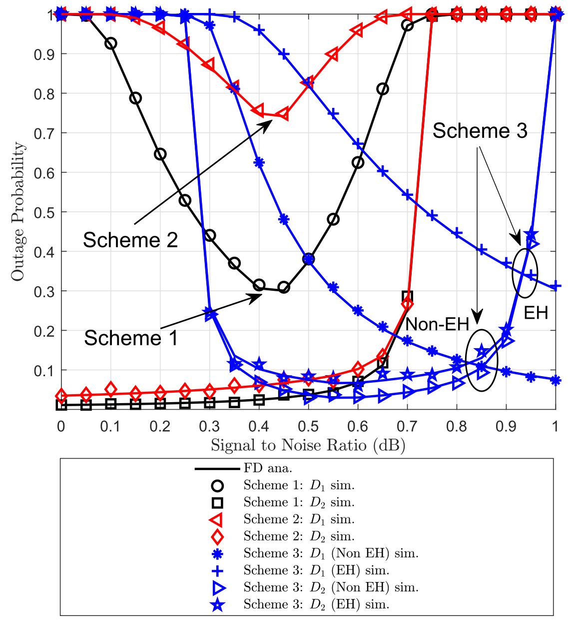

FIGURE 21. Comparison between the outage probability of the different schemes against a_1 when $\lambda_{g1,n} = 1$, $\lambda_{gn,k} = 5$, $\lambda_{h1} = 4$, $\lambda_{h2} = 1$, $\lambda_{hD1} = \lambda_{hr_k} = 0.01$, $R_1 = R_2 = 0.4$ BPCU, $\beta = \eta = 0.6$, and $N = K = 2$.

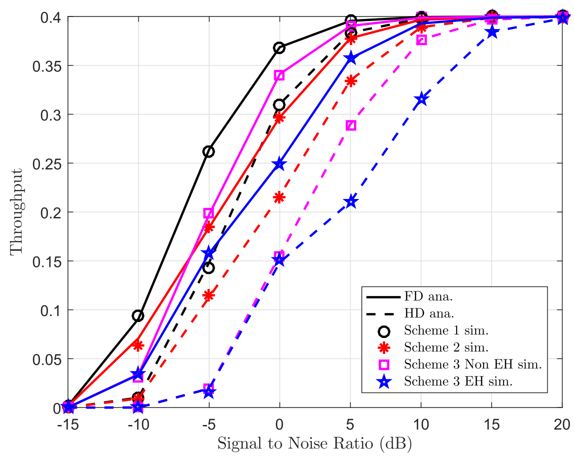

FIGURE 22. Comparison of the system throughput of the three schemes versus SNR when $\lambda_{g1,n} = 1$, $\lambda_{gn,k} = 5$, $\lambda_{h1} = 4$, $\lambda_{h2} = 1$, $\lambda_{hD1} = \lambda_{hr_k} = 0.01$, $R_1 = R_2 = 0.2$ BPCU, $\beta = \eta = 0.6$, and $N = K = 2$.

$a_2 > \varepsilon_2^l a_1$ and $a_1 > \varepsilon_1^l a_2$, $l = \{FD, HD\}$, in both FD and HD mode. It is noticed that all three proposed schemes have good throughput when the SNR is high. Furthermore, the FD mode achieves higher throughput than the HD mode while Scheme 1 shows the best performance.

V. CONCLUSION

In this paper, three novel FD cooperative relaying NOMA schemes for D2D communications have been proposed and analyzed. Precisely, closed form outage probability and throughput expressions for the proposed schemes have been evaluated. Monte-Carlo simulations results were presented to corroborate the derived analytical results. It was shown that the proposed schemes can significantly improve the outage performance compared to conventional OMA schemes where Scheme 1 achieves the best performance. Additionally, the combination of relaying with energy harvesting has brought great performance improvement to the system. Finally, interestingly, it has shown that the outage performance of FD NOMA is better than its HD counterpart.

APPENDIX A
PROOF OF THE THEOREM 2

From the expression (34), we can be obtained as

$$OP_{2-NOMA}^{FD} = \underbrace{\left[1-\Pr\left(\min\left(\gamma_{SD1\leftarrow 2}^{NOMA},\gamma_{D12,x2}^{NOMA}\right)\geq\varepsilon_2^{FD}\right)\right]}_{A} \times \underbrace{\prod_{k=1}^{K}\left(1-\Pr\left(\min\left(\gamma_{SRK,x2}^{NOMA},\gamma_{RKD2,x2}^{NOMA}\right)\geq\varepsilon_2^{FD}\right)\right)}_{B}, \tag{A.1}$$

where the first term of probability in (A.1) is calculated as (A.2).

Similarly, the second term of probability in (A.1) can be expressed as (A.3).

It is noted that the (A.2) and (A.3) can be obtained by the condition of $a_2 > \varepsilon_2^{FD} a_1$. The proof is completed.

APPENDIX B
PROOF OF THE THEOREM 3

The expression (38) can be expressed as (B.1).

From the first term of the expression in (B.1), we can rewrite:

$$\begin{aligned} M &= 1-\Pr\left(\gamma_{SD1\leftarrow 2}^{NOMA-EH}\geq\varepsilon_2^{FD},\gamma_{D12,x2}^{NOMA-EH}\geq\varepsilon_2^{FD}\right)\\ &= 1-\underbrace{\Pr\left(\gamma_{SD1\leftarrow 2}^{NOMA-EH}\geq\varepsilon_2^{FD}\right)}_{M_1}\underbrace{\Pr\left(\gamma_{D12,x2}^{NOMA-EH}\geq\varepsilon_2^{FD}\right)}_{M_2}, \end{aligned} \tag{B.2}$$

$$\begin{aligned} A &= 1-\Pr\left(\gamma_{SD1\leftarrow 2}^{NOMA}\geqslant\varepsilon_2^{FD}\right)\times\Pr\left(\gamma_{D12,x2}^{NOMA}\geqslant\varepsilon_2^{FD}\right)\\ &= 1-\Pr\left(|g_{1,n^*}|^2\geqslant\frac{\varepsilon_2^{FD}\omega\rho|h_{D1}|^2+\varepsilon_2^{FD}}{a_2\rho-\varepsilon_2^{FD}a_1\rho}\right)\times\Pr\left(|h_1|^2\geqslant\frac{\varepsilon_2^{FD}}{\rho}\right)\\ &= 1-\exp\left(-\frac{\varepsilon_2^{FD}}{\rho\lambda_{h1}}\right)\times\int_0^\infty\left(1-F_{|g_{1,n^*}|^2}\left(\frac{\varepsilon_2^{FD}\omega\rho x+\varepsilon_2^{FD}}{a_2\rho-\varepsilon_2^{FD}a_1\rho}\right)\right)f_{|h_{D1}|^2}(x)\,dx\\ &= 1-\sum_{n=1}^{N}\binom{N}{n}(-1)^{n-1}\frac{1}{\lambda_{D1}}\exp\left(-\frac{n\varepsilon_2^{FD}}{(a_2\rho-\varepsilon_2^{FD}a_1\rho)\lambda_{g1,n}}-\frac{\varepsilon_2^{FD}}{\rho\lambda_{h1}}\right)\int_0^\infty\exp\left(-\left(\frac{n\varepsilon_2^{FD}\omega\rho}{(a_2\rho-\varepsilon_2^{FD}a_1\rho)\lambda_{g1,n}}+\frac{1}{\lambda_{D1}}\right)x\right)dx\\ &= 1-\sum_{n=1}^{N}\binom{N}{n}(-1)^{n-1}\frac{(a_2\rho-\varepsilon_2^{FD}a_1\rho)\lambda_{g1,n}}{n\varepsilon_2^{FD}\omega\rho\lambda_{D1}+(a_2\rho-\varepsilon_2^{FD}a_1\rho)\lambda_{g1,n}}\exp\left(-\frac{n\varepsilon_2^{FD}}{(a_2\rho-\varepsilon_2^{FD}a_1\rho)\lambda_{g1,n}}-\frac{\varepsilon_2^{FD}}{\rho\lambda_{h1}}\right) \end{aligned} \tag{A.2}$$

$$\begin{aligned} B &= \prod_{k=1}^{K}\left(1-\Pr\left(\frac{a_2\rho|g_{n^*,k}|^2}{a_1\rho|g_{n^*,k}|^2+\omega\rho|h_{r_k}|^2+1}\geq\varepsilon_2^{FD},\rho|h_2|^2\geq\varepsilon_2^{FD}\right)\right)\\ &= \prod_{k=1}^{K}\left(1-\Pr\left(|g_{n^*,k}|^2\geq\frac{\varepsilon_2^{FD}\left(\omega\rho|h_{r_k}|^2+1\right)}{a_2\rho-\varepsilon_2^{FD}a_1\rho}\right)\times\Pr\left(|h_2|^2\geq\frac{\varepsilon_2^{FD}}{\rho}\right)\right)\\ &= \prod_{k=1}^{K}\left(1-\exp\left(-\frac{\varepsilon_2^{FD}}{\rho\lambda_{h2}}\right)\int_0^\infty\left(1-F_{|g_{n^*,k}|^2}\left(\frac{\varepsilon_2^{FD}(\omega\rho x+1)}{a_2\rho-\varepsilon_2^{FD}a_1\rho}\right)\right)f_{|h_{r_k}|^2}(x)\,dx\right)\\ &= \prod_{k=1}^{K}\left(1-\exp\left(-\frac{\varepsilon_2^{FD}}{\rho\lambda_{h2}}\right)\int_0^\infty\sum_{n=1}^{N}\binom{N}{n}(-1)^{n-1}\exp\left(-\frac{n\varepsilon_2^{FD}(\omega\rho x+1)}{(a_2\rho-\varepsilon_2^{FD}a_1\rho)\lambda_{gn,k}}\right)\frac{1}{\lambda_{hr_k}}\exp\left(-\frac{x}{\lambda_{hr_k}}\right)dx\right)\\ &= \prod_{k=1}^{K}\left(1-\sum_{n=1}^{N}\binom{N}{n}(-1)^{n-1}\frac{1}{\lambda_{hr_k}}\exp\left(-\frac{n\varepsilon_2^{FD}}{(a_2\rho-\varepsilon_2^{FD}a_1\rho)\lambda_{gn,k}}-\frac{\varepsilon_2^{FD}}{\rho\lambda_{h2}}\right)\int_0^\infty\exp\left(-\left(\frac{n\varepsilon_2^{FD}\omega\rho}{(a_2\rho-\varepsilon_2^{FD}a_1\rho)\lambda_{gn,k}}+\frac{1}{\lambda_{hr_k}}\right)x\right)dx\right)\\ &= \prod_{k=1}^{K}\left[1-\sum_{n=1}^{N}\binom{N}{n}(-1)^{n-1}\frac{(a_2-\varepsilon_2^{FD}a_1)\rho\lambda_{gn,k}}{n\varepsilon_2^{FD}\omega\lambda_{hr_k}+(a_2-\varepsilon_2^{FD}a_1)\rho\lambda_{gn,k}}\exp\left(-\frac{n\varepsilon_2^{FD}}{(a_2-\varepsilon_2^{FD}a_1)\rho\lambda_{gn,k}}-\frac{\varepsilon_2^{FD}}{\rho\lambda_{h2}}\right)\right] \end{aligned} \tag{A.3}$$

where the first term of the probability expression in (B.2) is calculated as (B.3) and the second term can be expressed as (B.4).

It is noted that the (B.3) and (B.4) can be obtained by the condition of $a_2 > \varepsilon_2^{FD} a_1$ and $|h_{D1}|^2 < \frac{1}{\eta\beta}$, respectively.

By substituting (B.3) and (B.4) into (B.2) and combine with (A.3), the proof is completed.

APPENDIX C
PROOF OF THE THEOREM 5

Substituting the expresstion (21) in to (40), the outage probability at D_1 in the case of QMFR Non-EH is calculated as (C.1).

Besides, implementing the same calculations for the case of QMFR EH, the outage probability at D_1 in the case of QMFR EH is obtained as (C.2). With some simple calculations for the expressions (C.1), (C.2) and combine with condition of $a_1 > \varepsilon_1^{FD} a_2$, the proof is complete.

APPENDIX D
PROOF OF THE THEOREM 6

The expression (44) can be rewritten as (D.1). Furthermore, the expressions E and F in (D.1) can be expressed as (D.2) and (D.3), respectively.

$$
\begin{aligned}
OP_{2-NOMA}^{FD-EH} &= \Pr\left(\min\left(\gamma_{SD1\leftarrow 2}^{NOMA-EH}, \gamma_{D12,x2}^{NOMA-EH}\right) < \varepsilon_2^{FD}\right) \times \Pr\left(\max_{k=1,\cdots,K} \min\left(\gamma_{SRK,x2}^{NOMA}, \gamma_{RKD2,x2}^{NOMA}\right) < \varepsilon_2^{FD}\right) \\
&= \underbrace{\left[1 - \Pr\left(\min\left(\gamma_{SD1\leftarrow 2}^{NOMA-EH}, \gamma_{D12,x2}^{NOMA-EH}\right) \geq \varepsilon_2^{FD}\right)\right]}_{M} \times \underbrace{\prod_{k=1}^{K}\left(1 - \Pr\left(\min\left(\gamma_{SRK,x2}^{NOMA}, \gamma_{RKD2,x2}^{NOMA}\right) \geq \varepsilon_2^{FD}\right)\right)}_{B}
\end{aligned} \tag{B.1}
$$

$$
\begin{aligned}
M_1 &= \Pr\left(|g_{1,n*}|^2 \geq \frac{\varepsilon_2^{FD}\omega\rho|h_{D1}|^2 + \varepsilon_2^{FD}}{\rho(1-\beta)\left(a_2 - a_1\varepsilon_2^{FD}\right)}\right) \\
&= \int_0^\infty \left(1 - F_{|g_{1,n*}|^2}\left(\frac{\varepsilon_2^{FD}\omega\rho x + \varepsilon_2^{FD}}{\rho(1-\beta)\left(a_2 - a_1\varepsilon_2^{FD}\right)}\right)\right) f_{|h_{D1}|^2}(x)\,dx \\
&= \int_0^\infty \sum_{n=1}^{N}\binom{K}{n}(-1)^{n-1}\exp\left(-\frac{n\left(\varepsilon_2^{FD}\omega\rho x + \varepsilon_2^{FD}\right)}{(1-\beta)\left(a_2 - a_1\varepsilon_2^{FD}\right)\rho\lambda_{1,n}}\right)\frac{1}{\lambda_{D1}}\exp\left(-\frac{x}{\lambda_{D1}}\right)dx \\
&= \sum_{n=1}^{N}\binom{K}{n}(-1)^{n-1}\frac{1}{\lambda_{D1}}\exp\left(-\frac{n\varepsilon_2^{FD}}{(1-\beta)\left(a_2 - a_1\varepsilon_2^{FD}\right)\rho\lambda_{1,n}}\right)\int_0^\infty \exp\left(-\left(\frac{n\varepsilon_2^{FD}\omega\rho}{(1-\beta)\left(a_2 - a_1\varepsilon_2^{FD}\right)\rho\lambda_{1,n}} + \frac{1}{\lambda_{D1}}\right)x\right)dx \\
&= \sum_{n=1}^{N}\binom{K}{n}(-1)^{n-1}\frac{(1-\beta)\left(a_2 - a_1\varepsilon_2^{FD}\right)\rho\lambda_{1,n}}{n\varepsilon_2^{FD}\omega\rho\lambda_{D1} + (1-\beta)\left(a_2 - a_1\varepsilon_2^{FD}\right)\rho\lambda_{1,n}}\exp\left(-\frac{n\varepsilon_2^{FD}}{(1-\beta)\left(a_2 - a_1\varepsilon_2^{FD}\right)\rho\lambda_{1,n}}\right)
\end{aligned} \tag{B.3}
$$

$$
\begin{aligned}
M_2 &= \Pr\left(|g_{1,n^*}|^2 \geq \frac{\varepsilon_2^{FD}\left(1 - \eta\beta|h_{D1}|^2\right)}{\eta\beta\rho|h_1|^2}\right) \\
&= \int_0^\infty \int_0^{\frac{1}{\eta}} \sum_{n=1}^{N}\binom{N}{n}(-1)^{n-1}\exp\left(-\frac{n\varepsilon_2^{FD}(1-\eta\beta x)}{\eta\beta\rho y\lambda_{g1,n}}\right)\frac{1}{\lambda_{D1}}\exp\left(-\frac{x}{\lambda_{D1}}\right)\frac{1}{\lambda_{h1}}\exp\left(-\frac{y}{\lambda_{h1}}\right)dxdy \\
&= \sum_{n=1}^{N}\binom{N}{n}(-1)^{n-1}\frac{1}{\lambda_{D1}}\frac{1}{\lambda_{h1}}\int_0^\infty\int_0^{\frac{1}{\eta}}\exp\left(\frac{n\varepsilon_2^{FD}x}{\rho y\lambda_{g1,n}} - \frac{x}{\lambda_{D1}}\right)\exp\left(-\frac{n\varepsilon_2^{FD}}{\eta\beta\rho y\lambda_{g1,n}} - \frac{y}{\lambda_{h1}}\right)dxdy \\
&= \sum_{n=1}^{N}\binom{N}{n}(-1)^{n-1}\frac{1}{\lambda_{h1}}\int_0^\infty \frac{\rho y\lambda_{g1,n}}{n\varepsilon_2^{FD}\lambda_{D1} + \rho y\lambda_{g1,n}}\left[\exp\left(\left(\frac{n\varepsilon_2^{FD}}{\rho y\lambda_{g1,n}} - \frac{1}{\lambda_{D1}}\right)\frac{1}{\eta}\right) - 1\right]\exp\left(-\frac{n\varepsilon_2^{FD}}{\eta\beta\rho y\lambda_{g1,n}} - \frac{y}{\lambda_{h1}}\right)dy \\
&= \sum_{n=1}^{N}\binom{N}{n}(-1)^{n-1}\frac{1}{\lambda_{h1}}\int_0^\infty \frac{\rho y\lambda_{g1,n}}{n\varepsilon_2^{FD}\lambda_{D1} + \rho y\lambda_{g1,n}}\left[\exp\left(-\left(\frac{1}{\beta} - 1\right)\frac{n\varepsilon_2^{FD}}{\eta\rho y\lambda_{g1,n}} - \frac{y}{\lambda_{h1}} - \frac{1}{\eta\lambda_{D1}}\right) - \exp\left(-\frac{n\varepsilon_2^{FD}}{\eta\beta\rho y\lambda_{g1,n}} - \frac{y}{\lambda_{h1}}\right)\right]dy
\end{aligned} \tag{B.4}
$$

According to (D.2), the expressions E_1 and E_2 can be calculated as follows, respectively.

$$E_1 = \Pr\left[\left|g_{1,n^*}\right|^2 \geq \left(\omega\rho|h_{D1}|^2+1\right) \times \max\left(\frac{\varepsilon_1^{FD}}{a_1\rho-\varepsilon_1^{FD}a_2\rho}, \frac{\varepsilon_2^{FD}}{a_2\rho}\right)\right] = \Pr\left[\left|g_{1,n^*}\right|^2 \geq \left(\omega\rho|h_{D1}|^2+1\right)\theta\right]$$

$$\begin{aligned} OP_{1-NOMA}^{FD-QMF} &= 1-\Pr\left(\left|g_{1,n^*}\right|^2 \geq \frac{\varepsilon_1^{FD}\omega\rho|h_{D1}|^2+\varepsilon_1^{FD}}{a_1\rho-\varepsilon_1^{FD}a_2\rho}\right) \\ &= 1-\int_0^\infty \sum_{n=1}^{N}\binom{N}{n}(-1)^{n-1}\exp\left(-\frac{n\left(\varepsilon_1^{FD}\omega\rho x+\varepsilon_1^{FD}\right)}{\left(a_1-\varepsilon_1^{FD}a_2\right)\rho\lambda_{g1,n}}\right)\frac{1}{\lambda_{hD1}}\exp\left(-\frac{x}{\lambda_{hD1}}\right)dx \\ &= 1-\sum_{n=1}^{N}\binom{N}{n}(-1)^{n-1}\frac{1}{\lambda_{hD1}}\exp\left(-\frac{n\varepsilon_1^{FD}}{\left(a_1-\varepsilon_1^{FD}a_2\right)\rho\lambda_{g1,n}}\right)\int_0^\infty \exp\left(-\left(\frac{n\varepsilon_1^{FD}\omega\rho}{\left(a_1-\varepsilon_1^{FD}a_2\right)\rho\lambda_{g1,n}}+\frac{1}{\lambda_{hD1}}\right)x\right)dx \end{aligned} \tag{C.1}$$

$$\begin{aligned} OP_{1-NOMA}^{FD-QMF-EH} &= 1-\Pr\left(\left|g_{1,n^*}\right|^2 \geq \frac{\varepsilon_1^{FD}\omega\rho|h_{D1}|^2+\varepsilon_1^{FD}}{(1-\beta)\left(a_1\rho-\varepsilon_1^{FD}a_2\rho\right)}\right) \\ &= 1-\int_0^\infty \sum_{n=1}^{N}\binom{N}{n}(-1)^{n-1}\exp\left(-\frac{n\left(\varepsilon_1^{FD}\omega\rho x+\varepsilon_1^{FD}\right)}{(1-\beta)\left(a_1-\varepsilon_1^{FD}a_2\right)\rho\lambda_{g1,n}}\right)\frac{1}{\lambda_{hD1}}\exp\left(-\frac{x}{\lambda_{hD1}}\right)dx \\ &= 1-\sum_{n=1}^{N}\binom{N}{n}(-1)^{n-1}\frac{1}{\lambda_{hD1}}\exp\left(-\frac{n\varepsilon_1^{FD}}{(1-\beta)\left(a_1-\varepsilon_1^{FD}a_2\right)\rho\lambda_{g1,n}}\right) \\ &\quad\times\int_0^\infty \exp\left(-\left(\frac{n\varepsilon_1^{FD}\omega\rho}{(1-\beta)\left(a_1-\varepsilon_1^{FD}a_2\right)\rho\lambda_{g1,n}}+\frac{1}{\lambda_{hD1}}\right)x\right)dx \end{aligned} \tag{C.2}$$

$$\begin{aligned} OP_{2-NOMA}^{FD-QMF} &= \underbrace{\left[1-\Pr\left(\gamma_{SD1}^{QMF}\geq\varepsilon_1^{FD},\gamma_{SD1,x2}^{QMF}\geq\varepsilon_2^{FD},\gamma_{D12,x2}^{NOMA}\geq\varepsilon_2^{FD}\right)\right]}_{E} \\ &\quad\times\underbrace{\prod_{k=1}^{K}\left(1-\Pr\left(\gamma_{SRK,x1}^{QMF}\geq\varepsilon_1^{FD},\gamma_{SRK,x2}^{QMF}\geq\varepsilon_2^{FD},\gamma_{RKD2,x2}^{NOMA}\geq\varepsilon_2^{FD}\right)\right)}_{F}. \end{aligned} \tag{D.1}$$

$$E = 1-\underbrace{\Pr\left(\gamma_{SD1}^{QMF}\geq\varepsilon_1^{FD},\gamma_{SD1,x2}^{QMF}\geq\varepsilon_2^{FD}\right)}_{E_1}\times\underbrace{\Pr\left(\gamma_{D12,x2}^{NOMA}\geq\varepsilon_2^{FD}\right)}_{E_2}. \tag{D.2}$$

$$F = \prod_{k=1}^{K}\left(1-\underbrace{\Pr\left(\gamma_{SRK,x1}^{QMF}\geq\varepsilon_1^{FD},\gamma_{SRK,x2}^{QMF}\geq\varepsilon_2^{FD},\gamma_{RKD2,x2}^{NOMA}\geq\varepsilon_2^{FD}\right)}_{F_1}\right) \tag{D.3}$$

$$\begin{aligned} OP_{2-NOMA}^{FD-QMF-EH} &= \underbrace{\left[1-\Pr\left(\gamma_{SD1}^{QMF-EH}\geq\varepsilon_1^{FD},\gamma_{SD1,x2}^{QMF-EH}\geq\varepsilon_2^{FD},\gamma_{D12,x2}^{NOMA-EH}\geq\varepsilon_2^{FD}\right)\right]}_{W} \\ &\quad\times\underbrace{\prod_{k=1}^{K}\left(1-\Pr\left(\gamma_{SRK,x1}^{QMF}\geq\varepsilon_1^{FD},\gamma_{SRK,x2}^{QMF}\geq\varepsilon_2^{FD},\gamma_{RKD2,x2}^{NOMA}\geq\varepsilon_2^{FD}\right)\right)}_{F} \end{aligned} \tag{E.1}$$

$$
\begin{aligned}
&= \sum_{n=1}^{N} \binom{N}{n} (-1)^{n-1} \frac{1}{\lambda_{hD1}} \\
&\quad \times \int_{0}^{\infty} \exp\left(-\frac{n\theta}{\lambda_{g1,n}}(\omega\rho x+1) - \frac{x}{\lambda_{hD1}}\right) dx \\
&= \sum_{n=1}^{N} \binom{N}{n} (-1)^{n-1} \frac{\lambda_{g1,n}}{n\theta\omega\rho\lambda_{hD1} + \lambda_{g1,n}} \\
&\quad \times \exp\left(-\frac{n\theta}{\lambda_{g1,n}}\right), \qquad \text{(D.4)}
\end{aligned}
$$

and

$$
\begin{aligned}
E_2 &= \Pr\left(\gamma_{D12,x2}^{NOMA} \geqslant \varepsilon_2^{FD}\right) \\
&= \Pr\left(|h_1|^2 \geqslant \frac{\varepsilon_2^{FD}}{\rho}\right) \\
&= \exp\left(-\frac{\varepsilon_2^{FD}}{\rho\lambda_{h1}}\right), \qquad \text{(D.5)}
\end{aligned}
$$

where $\theta = \max\left(\frac{\varepsilon_1^{FD}}{a_1\rho - \varepsilon_1^{FD} a_2 \rho}, \frac{\varepsilon_2^{FD}}{a_2\rho}\right)$ and with the condition of $a_1 > \varepsilon_1^{FD} a_2$.

Based on (D.3), the expression F_1 can be expressed as

$$
F_1 = \underbrace{\Pr\left(\gamma_{SRK,x1}^{QMF} \geq \varepsilon_1^{FD}, \gamma_{SRK,x2}^{QMF} \geq \varepsilon_2^{FD}\right)}_{F_2} \times \underbrace{\Pr\left(\gamma_{RKD2,x2}^{NOMA} \geq \varepsilon_2^{FD}\right)}_{F_3}. \qquad \text{(D.6)}
$$

In addition, the expressions F_2 and F_3 can be calculated as, respectively.

$$
\begin{aligned}
F_2 &= \Pr\left(\left|g_{n^*,k}\right|^2 \geq \left(\omega\rho\left|h_{r_k}\right|^2 + 1\right)\theta\right) \\
&= \sum_{n=1}^{N} \binom{N}{n} (-1)^{n-1} \frac{1}{\lambda_{hr_k}} \\
&\quad \times \int_{0}^{\infty} \exp\left(-\frac{n\theta}{\lambda_{gn,k}}(\omega\rho x+1) - \frac{x}{\lambda_{hr_k}}\right) dx \\
&= \sum_{n=1}^{N} \binom{N}{n} (-1)^{n-1} \frac{\lambda_{gn,k}}{n\theta\omega\rho\lambda_{hr_k} + \lambda_{gn,k}} \\
&\quad \times \exp\left(-\frac{n\theta}{\lambda_{gn,k}}\right), \qquad \text{(D.7)}
\end{aligned}
$$

in which the condition of $a_1 > \varepsilon_1^{FD} a_2$ still is maintained.

$$
\begin{aligned}
F_3 &= \Pr\left(\gamma_{RKD2,x2}^{NOMA} \geqslant \varepsilon_2^{FD}\right) \\
&= \Pr\left(|h_2|^2 \geqslant \frac{\varepsilon_2^{FD}}{\rho}\right) \\
&= \exp\left(-\frac{\varepsilon_2^{FD}}{\rho\lambda_{h2}}\right). \qquad \text{(D.8)}
\end{aligned}
$$

Substituting (D.1) and (D.5) into (D.2) and substituting (D.7) and (D.8) into (D.6), then combine with (D.3), the proof is completed.

APPENDIX E
PROOF OF THE THEOREM 7

The expression (46) can be rewritten as (E.1). Besides, the expressions W in (E.1) can be expressed as (E.2).

$$
W = 1 - \underbrace{\Pr\left(\gamma_{SD1}^{QMF-EH} \geq \varepsilon_1^{FD}, \gamma_{SD1,x2}^{QMF-EH} \geq \varepsilon_2^{FD}\right)}_{W_1} \times \underbrace{\Pr\left(\gamma_{D12,x2}^{NOMA-EH} \geq \varepsilon_2^{FD}\right)}_{M_2}, \qquad \text{(E.2)}
$$

where,

$$
\begin{aligned}
W_1 &= \Pr\left[\left|g_{1,n^*}\right|^2 \geq \left(\omega\rho|h_{D1}|^2 + 1\right)\zeta\right] \\
&= \sum_{n=1}^{N} \binom{N}{n} (-1)^{n-1} \frac{1}{\lambda_{hD1}} \exp\left(-\frac{n\zeta}{\lambda_{g1,n}}\right) \\
&\quad \times \int_0^{\infty} \exp\left(-\left(\frac{n\zeta\omega\rho}{\lambda_{g1,n}} + \frac{1}{\lambda_{hD1}}\right)x\right) dx \\
&= \sum_{n=1}^{N} \binom{N}{n} (-1)^{n-1} \\
&\quad \times \frac{\lambda_{g1,n}}{n\zeta\omega\rho\lambda_{hD1} + \lambda_{g1,n}} \exp\left(-\frac{n\zeta}{\lambda_{g1,n}}\right). \qquad \text{(E.3)}
\end{aligned}
$$

Substituting (E.3) and (B.4) into (E.2), then combine with (D.3), the proof is completed.

REFERENCES

[1] Y. Liu, Z. Qin, M. Elkashlan, Z. Ding, A. Nallanathan, and L. Hanzo, "Nonorthogonal multiple access for 5G and beyond," *Proc. IEEE*, vol. 105, no. 12, pp. 2347–2381, Dec. 2017.

[2] K. Yang, N. Yang, N. Ye, M. Jia, Z. Gao, and R. Fan, "Non-orthogonal multiple access: Achieving sustainable future radio access," *IEEE Commun. Mag.*, vol. 57, no. 2, pp. 116–121, Feb. 2019.

[3] X.-X. Nguyen and D.-T. Do, "Maximum harvested energy policy in full-duplex relaying networks with SWIPT," *Int. J. Commun. Syst.*, vol. 30, no. 17, p. e3359, Nov. 2017.

[4] Y. Saito, Y. Kishiyama, A. Benjebbour, T. Nakamura, A. Li, and K. Higuchi, "Non-orthogonal multiple access (NOMA) for cellular future radio access," in *Proc. IEEE 77th Veh. Technol. Conf. (VTC Spring)*, Jun. 2013, pp. 1–5.

[5] D. T. Do, H. S. Nguyen, M. Voznak, and T. S. Nguyen, "Wireless powered relaying networks under imperfect channel state information: System performance and optimal policy for instantaneous rate," *Radioengineering*, vol. 26, no. 3, pp. 869–877, Sep. 2017.

[6] X. Li, M. Liu, C. Deng, D. Zhang, X.-C. Gao, K. M. Rabie, and R. Kharel, "Joint effects of residual hardware impairments and channel estimation errors on SWIPT assisted cooperative NOMA networks," *IEEE Access*, vol. 7, pp. 135499–135513, 2019.

[7] D.-T. Do and M.-S. Van Nguyen, "Device-to-device transmission modes in NOMA network with and without wireless power transfer," *Comput. Commun.*, vol. 139, pp. 67–77, May 2019.

[8] G. Nauryzbayev, M. Abdallah, and K. M. Rabie, "On the reliability of decode-and-forward two-relay diversity-enabled NOMA networks," in *Proc. IEEE Wireless Commun. Netw. Conf. Workshop (WCNCW)*, Apr. 2019, pp. 1–6.

[9] Z. Ding, H. Dai, and H. V. Poor, "Relay selection for cooperative NOMA," *IEEE Wireless Commun. Lett.*, vol. 5, no. 4, pp. 416–419, Aug. 2016.

[10] J.-B. Kim, M. S. Song, and I.-H. Lee, "Achievable rate of best relay selection for non-orthogonal multiple access-based cooperative relaying systems," in *Proc. Int. Conf. Inf. Commun. Technol. Converg. (ICTC)*, Oct. 2016, pp. 960–962.

[11] S. Lee, D. B. da Costa, Q.-T. Vien, T. Q. Duong and R. T. de Sousa, "Outage probability of non-orthogonal multiple access schemes with partial relay selection," *IET Commun.*, Vol. 11, no. 6, pp. 846–854, 2017.

[12] X. Yue, Y. Liu, S. Kang, and A. Nallanathan, "Performance analysis of NOMA with fixed gain relaying over Nakagami-*m* fading channels," *IEEE Access*, vol. 5, pp. 5445–5454, 2017.

[13] D. Wan, M. Wen, F. Ji, Y. Liu, and Y. Huang, "Cooperative NOMA systems with partial channel state information over Nakagami-*m* fading channels," *IEEE Trans. Commun.*, vol. 66, no. 3, pp. 947–958, Mar. 2018.

[14] M. Ashraf, A. Shahid, J. W. Jang, and K.-G. Lee, "Energy harvesting non-orthogonal multiple access system with multi-antenna relay and base station," *IEEE Access*, vol. 5, pp. 17660–17670, 2017.

[15] Z. Ding, P. Fan, and H. V. Poor, "On the coexistence between full-duplex and NOMA," *IEEE Wireless Commun. Lett.*, vol. 7, no. 5, pp. 692–695, Oct. 2018.

[16] M. F. Kader, S. Y. Shin, and V. C. M. Leung, "Full-duplex non-orthogonal multiple access in cooperative relay sharing for 5G systems," *IEEE Trans. Veh. Technol.*, vol. 67, no. 7, pp. 5831–5840, Jul. 2018.

[17] L. Zhang, J. Liu, M. Xiao, G. Wu, Y.-C. Liang, and S. Li, "Performance analysis and optimization in downlink NOMA systems with cooperative full-duplex relaying," *IEEE J. Sel. Areas Commun.*, vol. 35, no. 10, pp. 2398–2412, Oct. 2017.

[18] X. Yue, Y. Liu, S. Kang, A. Nallanathan, and Z. Ding, "Exploiting Full/Half-duplex user relaying in NOMA systems," *IEEE Trans. Commun.*, vol. 66, no. 2, pp. 560–575, Feb. 2018.

[19] J. An, K. Yang, J. Wu, N. Ye, S. Guo, and Z. Liao, "Achieving sustainable ultra-dense heterogeneous networks for 5G," *IEEE Commun. Mag.*, vol. 55, no. 12, pp. 84–90, Dec. 2017.

[20] X. Lin, J. Andrews, A. Ghosh, and R. Ratasuk, "An overview of 3GPP device-to-device proximity services," *IEEE Commun. Mag.*, vol. 52, no. 4, pp. 40–48, Apr. 2014.

[21] P. Mach, Z. Becvar, and T. Vanek, "In-band device-to-device communication in OFDMA cellular networks: A survey and challenges," *IEEE Commun. Surveys Tuts.*, vol. 17, no. 4, pp. 1885–1922, Jun. 2015.

[22] J. Zhao, Y. Liu, K. K. Chai, Y. Chen, M. Elkashlan, and J. Alonso-Zarate, "NOMA-based D2D communications: Towards 5G," in *Proc. IEEE Global Commun. Conf. (GLOBECOM)*, Dec. 2016, pp. 1–6.

[23] Z. Zhang, Z. Ma, M. Xiao, Z. Ding, and P. Fan, "Full-duplex device-to-device-aided cooperative nonorthogonal multiple access," *IEEE Trans. Veh. Technol.*, vol. 66, no. 5, pp. 4467–4471, May 2017.

[24] J. Zhao, Y. Liu, K. K. Chai, Y. Chen, and M. Elkashlan, "Joint subchannel and power allocation for NOMA enhanced D2D communications," *IEEE Trans. Commun.*, vol. 65, no. 11, pp. 5081–5094, Nov. 2017.

[25] T. Yoon, T. H. Nguyen, X. T. Nguyen, D. Yoo, B. Jang, and V. D. Nguyen, "Resource allocation for NOMA-based D2D systems coexisting with cellular networks," *IEEE Access*, vol. 6, pp. 66293–66304, 2018.

[26] L. Wei, R. Hu, Y. Qian, and G. Wu, "Enable device-to-device communications underlaying cellular networks: Challenges and research aspects," *IEEE Commun. Mag.*, vol. 52, no. 6, pp. 90–96, Jun. 2014.

[27] C. Joo and S. Kang, "Joint scheduling of data transmission and wireless power transfer in multi-channel device-to-device networks," *J. Commun. Netw.*, vol. 19, no. 2, pp. 180–188, Apr. 2017.

[28] K. Guo, S. Dai, and G. Ascheid, "D2D underlaying massive MIMO TWRN with opportunistic energy harvesting," *IEEE Wireless Commun. Lett.*, vol. 6, no. 4, pp. 554–557, Aug. 2017.

[29] B. Chen, J. Liu, X. Yang, L. Xie, and Y. Li, "Resource allocation for energy harvesting-powered D2D communications underlaying NOMA-based networks," *IEEE Access*, vol. 7, pp. 61442–61451, 2019.

[30] Z. Kuang, G. Liu, G. Li, and X. Deng, "Energy efficient resource allocation algorithm in energy harvesting-based D2D heterogeneous networks," *IEEE Internet Things J.*, vol. 6, no. 1, pp. 557–567, Feb. 2019.

[31] J. Chen, J. Jia, Y. Liu, X. Wang, and A. H. Aghvami, "Optimal resource block assignment and power allocation for D2D-enabled NOMA communication," *IEEE Access*, vol. 7, pp. 90023–90035, 2019.

[32] Y. Xu, G. Wang, B. Li, and S. Jia, "Performance of D2D aided uplink coordinated direct and relay transmission using NOMA," *IEEE Access*, vol. 7, pp. 151090–151102, 2019.

[33] Z. Yang, Z. Ding, P. Fan, and N. Al-Dhahir, "The impact of power allocation on cooperative non-orthogonal multiple access networks with SWIPT," *IEEE Trans. Wireless Commun.*, vol. 16, no. 7, pp. 4332–4343, Jul. 2017.

[34] N.-P. Nguyen, T. Q. Duong, H. Q. Ngo, Z. Hadzi-Velkov, and L. Shu, "Secure 5G wireless communications: A joint relay selection and wireless power transfer approach," *IEEE Access*, vol. 4, pp. 3349–3359, 2016.

HUU-PHUC DANG received the B.S. degree in electrical electronics engineering from the HCMC University of Technology and Education, Vietnam, in 2004, and the M.Eng. degree in automation control from the Ho Chi Minh City University of Transport, Vietnam, 2012. He is currently pursuing the Ph.D. degree with the Ho Chi Minh City University of Technology and Education, Vietnam. He is also working at Tra Vinh University. His research interest includes signal processing in wireless communications networks and automation control.

MINH-SANG VAN NGUYEN was born in Bentre, Vietnam. He is currently pursuing the master's degree in the field of wireless communications with Industrial University of Ho Chi Minh City, Vietnam. He has worked closely with Dr. Thuan at the Wireless Communications and Signal Processing Research Group, Industrial University of Ho Chi Minh City. His research interests include electronic design, signal processing in wireless communications networks, non-orthogonal multiple access, and physical layer security.

DINH-THUAN DO received the B.S., M.Eng., and Ph.D. degrees from Vietnam National University (VNU-HCM), in 2003, 2007, and 2013, respectively, all in communications engineering. He was a Visiting Ph.D. Student with the Communications Engineering Institute, National Tsing Hua University, Taiwan, from 2009 to 2010. Prior to joining Ton Duc Thang University, he was a Senior Engineer at VinaPhone Mobile Network, from 2003 to 2009. He has published over 65 SCI/SCIE journal papers. His research interests include signal processing in wireless communications networks, cooperative communications, non-orthogonal multiple access, full-duplex transmission, and energy harvesting. He was a recipient of the Golden Globe Award from the Vietnam Ministry of Science and Technology (Top 10 excellent young scientists nationwide), in 2015. He served as a Lead Guest Editor for special issue "Recent Advances for 5G: Emerging Scheme of NOMA in Cognitive Radio and Satellite Communications" in Electronics. He is currently serving as an Associate Editor of *EURASIP Journal on Wireless Communications and Networking*, *Computer Communications* (Elsevier), *Electronics*, and *KSII Transactions on Internet and Information Systems*.

HONG-LIEN PHAM is currently working as an Associate Professor with the Ho Chi Minh City University of Technology and Education, Vietnam. Her research interests include telecommunications networks, computer networks, and digital signal processing in wireless communications networks.

BASSANT SELIM (Member, IEEE) received the master's degree in communication systems from Pierre et Marie Curie (Paris XI) University, Paris, France, in 2011, and the Ph.D. degree from Khalifa University, Abu Dhabi, United Arab Emirates, in 2017. She is currently a Postdoctoral Fellow at the École de Technologie Supérieure, Montreal, Canada. Her research interests include wireless communications, radio-frequency impairments, and non-orthogonal multiple access.

GEORGES KADDOUM received the bachelor's degree in electrical engineering from the École Nationale Supérieure de Techniques Avancées (ENSTA Bretagne), Brest, France, and the M.S. degree in telecommunications and signal processing (circuits, systems, and signal processing) from the Université de Bretagne Occidentale and Telecom Bretagne (ENSTB), Brest, in 2005, and the Ph.D. degree (Hons.) in signal processing and telecommunications from the National Institute of Applied Sciences (INSA), University of Toulouse, Toulouse, France, in 2009. He is currently an Associate Professor and a Tier 2 Canada Research Chair with the École de Technologie Supérieure (ÉTS), Université du Québec, Montréal, Canada. He has published over 200 journal and conference papers and has two pending patents. His recent research activities cover mobile communication systems, modulations, security, and space communications and navigation. He was awarded the ÉTS Research Chair in physical-layer security for wireless networks, in 2014, and the prestigious Tier 2 Canada Research Chair in wireless IoT networks, in 2019. Since 2010, he has been a Scientific Consultant in the field of space and wireless telecommunications for several U.S. and Canadian companies. He received the Best Papers Awards at the 2014 IEEE International Conference on Wireless and Mobile Computing, Networking, Communications (WIMOB), with three coauthors, and at the 2017 IEEE International Symposium on Personal Indoor and Mobile Radio Communications (PIMRC), with four coauthors. He also received the IEEE TRANSACTIONS ON COMMUNICATIONS Exemplary Reviewer Award for the year 2015 and 2017. In addition, he received the Research Excellence Award of the Université du Québec, in 2018, and the Research Excellence Award from the ÉTS in recognition of his outstanding research outcomes, in 2019. He is currently serving as an Associate Editor of the IEEE TRANSACTIONS ON INFORMATION FORENSICS AND SECURITY, and the IEEE COMMUNICATIONS LETTERS.